Interaction between induced and natural variation at *oil yellow1* delays reproductive maturity in maize

Rajdeep S. Khangura[†§‡], Bala P. Venkata[†2], Sandeep R. Marla[†1], Michael V. Mickelbart[†‡], Singha Dhungana[3], David M. Braun[3], Brian P. Dilkes[§‡], Gurmukh S. Johal[†‡]

[†]Department of Botany and Plant Pathology, Purdue University, West Lafayette, Indiana 47907

[‡]Center for Plant Biology, Purdue University, West Lafayette, Indiana 47907

[§]Department of Biochemistry, Purdue University, West Lafayette, Indiana 47907

[3]Division of Biological Sciences, Interdisciplinary Plant Group, Missouri Maize Center, University of Missouri, Columbia, Missouri 65211

Current address

[1]Department of Agronomy, Kansas State University, Manhattan, Kansas 66506

[2]Donald Danforth Plant Science Center, St. Louis, Missouri 63132

Corresponding Authors

Brian P. Dilkes, 170 S. University Street, Purdue University, West Lafayette, Indiana 47907, Phone: (765) 494 2584, Email: bdilkes@purdue.edu

Gurmukh S. Johal, 915 W. State Street, Purdue University, West Lafayette, Indiana 47907, Phone: (765) 494-4448, Email: gjohal@purdue.edu

Abstract

We previously demonstrated that maize (*Zea mays*) locus *very oil yellow1 (vey1)* encodes a putative cis-regulatory expression polymorphism at the magnesium chelatase subunit I gene (aka *oil yellow1*) that strongly modifies the chlorophyll content of the semi-dominant *Oy1-N1989* mutants. The *vey1* allele of Mo17 inbred line reduces chlorophyll content in the mutants leading to reduced photosynthetic output. *Oy1-N1989* mutants in B73 reached reproductive maturity four days later than wild-type siblings. Enhancement of *Oy1-N1989* by the Mo17 allele at the *vey1* QTL delayed maturity further, resulting in detection of a flowering time QTL in two bi-parental mapping populations crossed to *Oy1-N1989*. The near isogenic lines of B73 harboring the *vey1* allele from Mo17 delayed flowering of *Oy1-N1989* mutants by twelve days. Just as previously observed for chlorophyll content, *vey1* had no effect on reproductive maturity in the absence of the *Oy1-N1989* allele. Loss of chlorophyll biosynthesis in *Oy1-N1989* mutants and enhancement by *vey1* reduced CO_2 assimilation. We attempted to separate the effects of photosynthesis on the induction of flowering from a possible impact of chlorophyll metabolites and retrograde signaling by manually reducing leaf area. Removal of leaves, independent of the *Oy1-N1989* mutant, delayed flowering but surprisingly reduced chlorophyll contents of emerging leaves. Thus, defoliation did not completely separate the identity of the signal(s) that regulates flowering time from changes in chlorophyll content in the foliage. These findings illustrate the necessity to explore the linkage between metabolism and the mechanisms that connect it to flowering time regulation.

KEYWORDS flowering time; photosynthesis; epistasis, setaria; sorghum

46 **Introduction**

47 The onset of flowering in angiosperms has been a key focus for plant biologists working on
48 ornamental, horticultural, and other crop species (Lang 1952; Zeevaart 1962; Searle 1965). The
49 onset of reproductive development in angiosperms is affected by a change in meristem identity.
50 The vegetative to floral transition of meristems commits plant development to production of floral
51 organs and sexual reproduction. The integration of signals to correctly time this transition is key
52 to plant fitness. Unsurprisingly, endogenous and environmental cues regulate flowering time
53 (Amasino and Michaels 2010; Cho *et al.* 2017; Minow *et al.* 2018). A critical environmental cue
54 is the duration of the light period, or photoperiod. The photoperiodic responses of plants influence
55 the vegetative to floral transition and the mechanisms of this response have been a focus of
56 intensive research for over a century (Klebs, 1918). Multiple non-photoperiodic cues as well as
57 endogenous signals, sometimes called the autonomous pathway, are also critical to floral transition.
58 Endogenous signals, including hormones and the carbohydrate status of the plant, can also play a
59 critical role in the regulation of flowering time (Corbesier *et al.* 1998; Moghaddam and Ende 2013).
60 But it can be difficult to fully separate endogenous and environmental influences as some
61 environmental factors, such as light quality, alter hormone biosynthesis (Lang 1957; Evans and
62 Poethig 1995; Mutasa-Göttgens and Hedden 2009), and light powers photosynthesis and thereby
63 carbohydrate status (Chen *et al.* 2004). These stimuli converge through the same floral integrators
64 (named FLOWERING LOCUS T (FT) and FLOWERING LOCUS D (FD) in *Arabidopsis*
65 *thaliana)* for which orthologs have been identified in many flowering plants (Abe *et al.* 2005;
66 Wigge *et al.* 2005; Corbesier *et al.* 2007; Meng *et al.* 2011; Zhang *et al.* 2016). Accumulation of
67 FT and FD gene products trigger the vegetative shoot apical meristems to acquire the competency
68 to become inflorescence meristems and produce flowers in part via the activation of MADS-box
69 transcription factors that control meristem identity through APETALA1 (Abe *et al.* 2005; Wigge

70 *et al.* 2005). In Arabidopsis, FT is regulated by CONSTANS (CO) in response to both circadian
71 regulation and photoperiodic responses, and CO regulates the MADS-box transcription factor
72 SUPPRESSOR OF CONSTANS1 (SOC1) through FT (Samach *et al.* 2000; Yoo *et al.* 2005).

73 Maize was domesticated from teosinte (*Zea mays* ssp. *parviglumis* or spp. *mexicana*) in
74 Central America (Doebley *et al.* 1997; Wang *et al.* 1999). Strong selection on time to reproductive
75 maturity contributed to the adaptation of maize to different latitudes (Salvi *et al.* 2007; Huang *et*
76 *al.* 2017; Swarts *et al.* 2017). Flowering of teosinte is promoted by short-day conditions. In contrast,
77 temperate maize germplasm is relatively day-neutral and flowering is primarily under the control
78 of the autonomous pathway (Coles *et al.* 2010). Mutant studies have identified loci critical to
79 flowering in maize including: *indeterminate1* (*id1*; Colasanti et al. 1998); *early phase change* (*epc*;
80 Vega et al. 2002); *delayed flowering1* (*dlf1*; Muszynski et al. 2006); the cis-element polymorphism
81 *vegetative transitioning1* (*vgt1*; Salvi et al. 2007) that regulates a downstream APETALA2-like
82 transcription factor *zmrap2.7*; *zea mays mads4* (*zmm4*; Danilevskaya et al. 2008); *zmcct10* (Hung
83 *et al.* 2012); *zea mays centroradiales8* (*zcn8*; Meng et al. 2011); *zea mays mads1* (*zmmads1*; Alter
84 et al. 2016); and *zea mays mads69* (Liang *et al.* 2019). Many of these loci encode the maize
85 orthologs of genes identified as regulators of flowering in Arabidopsis. For example, *dlf1* and *zcn8*
86 encode homologs of the Arabidopsis flowering time determinants FD and FT, respectively. *id1*
87 encodes a zinc-finger transcription factor acting upstream of both DLF1 and ZCN8 (Kozaki *et al.*
88 2004; Muszynski *et al.* 2006; Meng *et al.* 2011). *zmm4* is an activator of flowering that is part of
89 a conserved syntenic pair of MADS box genes in the grasses, with *zmm24* as the neighboring gene,
90 and encodes one of two maize paralogs of the wheat flowering time and vernalization response
91 locus VRN1 (Danilevskaya *et al.* 2008). *zmm4* acts downstream of *dlf1* and *id1* in the control of
92 flowering time in maize. *zmmads1* is a functional homolog of the Arabidopsis flowering time and

93 circadian rhythm regulator *soc1* (Alter *et al.* 2016). Several QTL studies have used the convenient
94 phenotype of days to reproductive maturity as a proxy for flowering time and identified alleles
95 controlling this trait in maize (Buckler *et al.* 2009; Coles *et al.* 2010; Steinhoff *et al.* 2012; Bouchet
96 *et al.* 2017). While this trait is convenient it is determined by both the days to floral transition of
97 the meristem and the growth rate of the stem and emergence and maturation of floral structures.
98 Nevertheless, many natural variants controlling days to reproductive maturity in maize map to
99 *bona fide* flowering time loci identified by mutant studies including alleles of *zmmads69*, *zmcct10*,
100 *zcn8*, *dlf1*, and *vgt1* (Muszynski *et al.* 2006; Salvi *et al.* 2007; Meng *et al.* 2011; Hung *et al.* 2012;
101 Guo *et al.* 2018; Liang *et al.* 2019).

102 One important endogenous signal that contributes to flowering time is the carbohydrate
103 allocation status (Ohto *et al.* 2001; Seo *et al.* 2011; Eveland and Jackson 2012; Wahl *et al.* 2013;
104 Cho *et al.* 2018). In maize, mutants that are compromised in either sugar export from source tissues
105 or loading sucrose into the phloem flower later than their congenic wild-type siblings (Braun *et al.*
106 2006; Baker and Braun 2008; Ma *et al.* 2008; Slewinski *et al.* 2009; Slewinski and Braun 2010).
107 This is not limited to maize, as starch-deficient Arabidopsis mutants exhibit delayed flowering
108 (Corbesier *et al.* 1998). Trehalose-6-phosphate (T6P) has been implicated as a reporter of the
109 energy status and Arabidopsis mutants effected in this metabolite also exhibit altered flowering
110 time (Paul 2008; Wahl et al. 2013; Seo et al. 2011). T6P and sucrose are positively correlated, and
111 low levels of T6P results in delayed flowering in Arabidopsis (Wahl *et al.* 2013). Remarkably, the
112 carbohydrate status and transcriptional regulatory genes controlling flowering time may be directly
113 linked in maize. The *id1* flowering time mutants alter carbohydrate partitioning in leaves and
114 accumulate more sucrose and starch (Coneva et al. 2012). As a result, ID1 has been proposed to
115 act as a carbohydrate status sensor that influences flowering time in maize (Coneva, Zhu, and

116 Colasanti 2007; Minow et al. 2018). Remarkably, the promoter of the T6P biosynthetic gene
117 *trehalose 6-phosphate synthase1* (*tps1*) is a predicted target of the ID1 DNA-binding protein and
118 low levels of T6P were observed in *id1* mutants (Minow *et al.* 2018).

119 If sugars are critical for floral transitioning in plants, then manipulation of photosynthesis
120 should alter flowering. Magnesium chelatase (MgChl) is a hetero-oligomeric enzyme complex
121 comprised of subunits I, D, and H. This enzyme catalyzes the first committed step of chlorophyll
122 biosynthesis by conversion of protoporphyrin IX (PPIX) into magnesium-PPIX (Walker and
123 Weinstein 1991; Gibson et al. 1995). The I subunit of MgChl is encoded by *oil yellow1* (*oy1*) in
124 maize (Sawers *et al.* 2006). The OY1-N1989 mutant protein carries a L176F amino acid
125 substitution that results in the protein acting as a competitive inhibitor of MgChl complex function,
126 and decouples ATPase and Mg^{2+} chelatase activity (Hansson *et al.* 1999, 2002; Sawers *et al.* 2006).
127 As a result, homozygous *Oy1-N1989* mutants are seedling lethal with no chlorophyll accumulation
128 but are viable to reproductive maturity in heterozygous condition (Sawers *et al.* 2006, Khangura
129 *et al.* 2019).

130 We previously identified a cis-acting expression polymorphism at the *oy1* locus associated
131 with a QTL called *very oil yellow1* (*vey1*) that modifies the chlorophyll content of semi-dominant
132 *Oy1-N1989* mutants (Khangura *et al.* 2019). The *vey1* QTL was proposed to modulate the
133 chlorophyll content of heterozygous *Oy1-N1989/+* mutants via cis-regulatory differences resulting
134 in differential accumulation of the product encoded by the wild-type allele at *oy1*. The Mo17 allele
135 at *vey1* ($vey1^{Mo17}$) was associated with lower abundance of OY1 transcripts, whereas the B73 allele
136 at *vey1* ($vey1^{B73}$) is associated with higher accumulation of OY1. The effect of *vey1* on chlorophyll
137 content is only visible in the presence of *Oy1-N1989,* indicating that this natural variant has a
138 cryptic effect on the function of the MgChl complex.

139 In this study, we used controlled crosses to segregate *Oy1-N1989* and the modifier alleles at
140 *vey1* (*vey1*^{B73} and *vey1*^{Mo17}) to generate populations of maize with a range of chlorophyll contents.
141 We used this variation in chlorophyll to explore the effects of chlorophyll content on net CO_2
142 assimilation. These changes in chlorophyll accumulation resulted in changes in net CO_2
143 assimilation and photosynthetically-fixed carbon accumulation. Remarkably, we noticed that
144 flowering time across material with differing photosynthetic rates and chlorophyll contents was
145 dramatically different. We observed that reduced chlorophyll accumulation was associated with a
146 delay in flowering time. Similar to the cryptic effects of *vey1* on chlorophyll content, the modifier
147 allele had no effect on flowering time in the absence of the *Oy1-N1989* mutant allele. Chlorophyll
148 content was consistently associated with earlier flowering and partial rescue of chlorophyll
149 accumulation in the *Oy1-N1989* mutant by the *vey1* QTL accelerated flowering in the mutants but
150 had no effect on wild-type siblings. In addition to measurements of net CO_2 assimilation, the
151 premature senescence of maize leaves, induced by sugar accumulation following sink removal,
152 was also reduced by *Oy1-N1989* and further reduced by *vey1* alleles that decrease chlorophyll
153 content and net CO2 assimilation. The effect of reduced photosynthate accumulation on flowering
154 time was not specific to *Oy1-N1989* as mechanical removal of leaves, to reduce plant leaf area,
155 also delayed flowering time. Thus, all of our results are consistent with an integrative measure of
156 carbon assimilation linking energy status and flowering time in maize.

157 **Materials and Methods**

158 **Plant materials**

159 Our previously described stock of the *Oy1-N1989* mutant allele is maintained in the B73
160 background and is propagated by crossing heterozygous mutants (*Oy1-N1989/+*) to wild-type

161 siblings (Khangura *et al.* 2019). The B73 introgressed stock of *Oy1-N1989* was used for crossing
162 to various mapping populations. A total of 216 intermated B73 × Mo17 population (IBM-RILs),
163 and 251 synthetic 10 doubled haploid lines (Syn10-DH) were crossed as ear-parents with *Oy1-*
164 *N1989/*+:B73 pollen. The pollen of *Oy1-N1989/*+:B73 plants were also crossed on to the ears of
165 35 B73-Mo17 near-isogenic lines (BM-NILs) for QTL validation. Tables S1-S3 contain the full
166 list of IBM-RILs, Syn10-DH, and BM-NILs used to develop F_1 hybrid populations.

167 **Field trials**

168 All of the field experiments described in this study were conducted at the Purdue Agronomy Center
169 for Research and Education (ACRE) in West Lafayette, Indiana. Each cross was evaluated as a
170 single plot of 12-16 plants. Each plot derived from crosses with *Oy1-N1989/*+:B73 tester
171 segregated for both mutant and wild-type siblings in approximately 1:1 ratio. Seeds were sown
172 with a tractor-driven seed planter with plot length of 3.84 meters (m), alley length of 0.79 m, and
173 inter-row spacing of 0.79 m. Standard crop management practices at Purdue in terms of fertilizer,
174 pest, and weed control for growing field maize were adopted.

175 Each experiment was divided into blocks. Progenies from crosses of B73 and Mo17 ears to
176 *Oy1-N1989/*+:B73 pollen were used as parental checks in each block. Parental checks were
177 randomized within each block. The IBM-RILs F_1 populations were evaluated as a single
178 replication in 2013. Syn10-DH F_1 populations were evaluated in 2016 with two full replications
179 planted in randomized complete block design (RCBD). Hybrid progenies of *Oy1-N1989/*+:B73
180 with BM-NILs were screened in 2016 with five replications planted in RCBD.

181 **Field phenotyping and data collection**

182 The mutant plants in each plot were identified visually as pale plants. The chlorophyll content in
183 mutant and wild-type plants was approximated using a CCM-200 plus (Opti-Sciences Inc., Hudson,
184 NH) as described in Khangura *et al.* 2019. We previously demonstrated correlation of 0.94
185 between CCM-200 plus values and chlorophyll *a*, chlorophyll *b*, and total chlorophyll contents
186 (Khangura *et al.* 2019), and therefore used CCM-200 plus values (CCM) as a proxy for chlorophyll
187 content in the materials described here. CCMI refers to measurements taken with the CCM-200
188 plus instrument from 25-30 days after sowing and CCMII refers to measurements taken 45-50 days
189 after sowing. Mutants were tagged between the V5-V7 stages of development. Tagging is
190 necessary as suppression of the *Oy1-N1989* mutant phenotype by *vey1* interferes with visual
191 classification of mutant and wild-type siblings at maturity. Reproductive maturity in each F_1
192 population was recorded separately on the wild-type and mutant plants. The date at which roughly
193 half of the wild-type or mutant plants in a given plot were shedding pollen and had emerging silks
194 from the primary ear was recorded as the date of anthesis and date of silking, respectively, for a
195 given genotype. The dates of anthesis and silking for both wild-type and mutant genotypes were
196 then subtracted from the date of planting to obtain respective wild-type or mutant days to anthesis
197 (DTA), and days to silking (DTS). Further, the difference between DTA and DTS was used to
198 derive the anthesis-silking interval (ASI); ASI = DTA-DTS. Wild-type and mutant trait values are
199 denoted with a prefix WT and MT, respectively. Ratio and differences of these flowering time
200 traits were also calculated as MT/WT and WT-MT, respectively.

201 A total of 15 F_1 populations derived from B73-like NILs × *Oy1-N1989/+*:B73 cross were
202 used to study induced leaf senescence. Seven of these B73-like NILs carried an introgression of
203 *vey1* from Mo17 ($vey1^{Mo17}$), whereas the other eight NILs had the B73 genotype at *vey1* ($vey1^{B73}$).

204 These NIL populations were planted in the field with at least two replications of each genotype
205 planted in RCBD and two times separated by two weeks. The procedure for this experiment was
206 adapted from Sekhon *et al.* 2012. Briefly, primary and secondary ears of both wild-type and mutant
207 plants were covered with shoot bags before silk emergence. After 3-4 days of tassel shedding,
208 roughly half of the shoot bags were removed, and these ears were allowed to open pollinate.
209 Staggered rows of B73, in addition to the pollen shed within the row fully pollinated exposed ears.
210 The day of shoot exposure was marked as 0 days after anthesis (DAA). Photographs were taken
211 on the same date using plants from both planting dates to permit display of differences in the effect
212 of DAA on phenotype severity.

213 **Genotypic and gene expression data**

214 The genotypic data and other public datasets on various mapping populations used in this
215 study have been described previously (Khangura *et al.* 2019). Briefly, the public marker dataset
216 for IBM-RILs was obtained from MaizeGDB with 2,178 markers (Sen *et al.* 2010). The markers
217 were reduced to 2,156 after removing duplicate variants, with ~13.3 percent of missing data in the
218 final dataset. Genotypic data consisting of 6611 SNPs for Syn10-DH lines was obtained from Liu
219 et al. 2015. This dataset had no missing genotypes and was used as such for QTL analyses.
220 Genotypes of the B73-Mo17 Near Isogenic Lines (BM-NILs) used for QTL validation were
221 obtained from Eichten *et al.* 2011. Expression data of *oy1* locus in IBM-RILs were obtained from
222 a public repository of the National Science Foundation grant (GEPR: Genomic Analyses of shoot
223 meristem function in maize; NSF DBI-0820610;
224 https://download.maizegdb.org/GeneFunction_and_Expression/ShootApicalMeristem/). This
225 data consists of the expression of maize genes in the tissue derived from the shoot apex of 14 days

226 old IBM-RILs seedlings. The expression data from each gene is normalized to reads per kilobase
227 of transcript per million mapped reads (RPKM).

228 **Allele-specific expression (ASE) assay**

229 Three replications of B73-Mo17 near-isogenic lines (BM-NILs) × *Oy1-N1989/*+:B73 F_1 progenies
230 were grown in the field. Mutant siblings derived from four B73-like NILs crossed with *Oy1-*
231 *N1989/*+:B73 were selected for the ASE experiment. These NILs consisted of two B73-like NILs
232 (b094 and b189) with $vey1^{Mo17}$, and other two B73-like NILs (b135 and b185) with $vey1^{B73}$
233 genotype. Leaf tissue was harvested from the top fully-expanded leaf at the V3 developmental
234 stage from the mutant siblings of the four B73-like NIL F_1 plots. For each biological replicate,
235 tissue was pooled from 4-5 seedlings to make one sample. The samples were stored at -80 ˚C until
236 needed. The procedure of total RNA isolation, cDNA synthesis, and the ASE assay has been
237 described previously in detail (Khangura *et al.* 2019). Briefly, one µg of DNase treated total RNA
238 was used to synthesize cDNA. PCR was conducted using the forward oligonucleotide 5'-
239 TCACCGTCTGCAATGTCGCCGCTC -3' and reverse oligonucleotide 5'-
240 AGTATGCCCCTGTTGGCCTTGGCG -3' under following reaction conditions with 30 cycles of
241 polymerization (94˚C for 30s, 56˚C for 30s, 72 ˚C for 30s and final extension for 2 minutes) to
242 amplify the targeted region of OY1. The primer pair used in this assay flanked the SNP that causes
243 the L176F amino acid substitution in the *Oy1-N1989* mutant allele. PCR products were sequenced
244 on a MiSeq instrument (Illumina, San Diego, CA) at the Purdue Genomics Core Facility. Reads
245 were aligned to a small reference sequence of B73 derived from targeted PCR region using the
246 GATK packages (DePristo *et al.* 2011). Read counts derived from GATK was used to calculate
247 allele-specific expression. Genomic DNA derived from B73 × Mo17 F_1 hybrids resulted in roughly
248 1:1 read counts demonstrating no bias in the assay.

249 **Statistical analyses**

250 Exploratory data analysis was done using JMP 13.0 (SAS Institute Inc. 2016). The pairwise
251 correlations were calculated using the Pearson correlation coefficient. The average values of
252 various traits from line-cross populations, IBM-RILs and Syn10-DH, were subjected to QTL
253 analyses. QTL detection was done using a single interval mapping via the EM algorithm using the
254 function "scanone" in R/qtl, a software package implemented in R (Broman *et al.* 2003; R core
255 Team 2013). Similar results were obtained with composite interval mapping function "cim" in
256 R/qtl (data not shown).

257 **Defoliation assay**

258 The defoliation experiments were performed using maize inbred B73, sorghum (*Sorghum bicolor*)
259 inbred BTx623, and green foxtail (*Setaria viridis*) inbred A10.1. These experiments were
260 conducted in a greenhouse using mogul base high-pressure sodium lamps (1000 Watts) as the
261 supplemental light source for L:D cycle of 16:8 hours, with the temperature set at 28ºC (day-time)
262 and 20ºC (night-time). The maize inbred line B73 was defoliated at V3 leaf stage. All the leaves
263 with a fully visible leaf collar were cut slightly above the ligule. Sorghum plants with three to four
264 fully opened leaves (~20 days after sowing in the greenhouse) were defoliated in a similar way.
265 All fully expanded leaves at ~15 days after planting, including those on tillers, were removed in
266 *Setaria* plants. The time to reproductive maturity of both defoliated and undisturbed controls was
267 recorded on maize as described above. For sorghum and *Setaria*, the date of head emergence,
268 rather than anthesis, on every plant was recorded and deducted from the date of planting to obtain
269 days to heading.

270 **Non-structural carbohydrate (NSC) quantification**

271 The soluble sugars and starch were quantified from the mutant siblings of four B73-NILs × *Oy1-*
272 *N1989/+*:B73 F_1 population. Two of these NILs carried *vey1*^{Mo17}, while the other two had *vey1*^{B73}
273 genotype. Plants were grown in the field with three replications using a RCBD. The top fully-
274 expanded leaf at the V3 stage was harvested at 1:00 PM and transferred to liquid nitrogen. Leaf
275 tissues were stored at -80°C until needed. Leaf samples were ground into a fine powder and ~100
276 mg of the powder was used to extract sucrose, glucose, fructose, and starch using a previously
277 described method (Leach and Braun 2016). The quantification of these NSC was done using a
278 previously described method (Leach *et al.* 2017). Briefly, high-performance anion exchange
279 (HPAE) chromatography (ICS-5000, Thermo-Fisher Scientific) was used to analyze the neutral
280 fraction of the extract. Sugar standards were used to construct a standard curve, and samples were
281 diluted to ensure that the detected values fell within the scope of this curve.

282 **Gas-exchange measurements**

283 Gas-exchange measurements were taken on field-grown plants during the summer of 2017 at the
284 Purdue ACRE farm. The gas-exchange measurements were taken on the third leaf on plants at the
285 V3 stage between 11 AM and 1 PM using a LICOR LI-6400XT open photosynthesis system (LI-
286 COR Inc., Lincoln, NE, USA). The F_1 progenies used for these measurements consisted of four
287 independent B73-NILs × *Oy1-N1989/+*:B73 cross, in which two NILs carried *vey1*^{Mo17}
288 introgression and the other two carried *vey1*^{B73} allele. Plants were grown in a RCBD of three
289 replicated blocks. For each genotype, nine plants were measured as three replicates in each of the
290 three blocks. The following instrument conditions were maintained throughout the measurement
291 period: an artificial light source with an intensity of 1700 µmol photosynthetically active radiation

292 (PAR) m^{-2} s^{-1}, air temperature of ~31 ºC, CO_2 concentration of 400 mL L^{-1}, air flow of 400 µmol
293 s^{-1}, and relative humidity of 50-60%. Leaf temperatures varied from 32-34ºC during the
294 measurements.

295 Chlorophyll fluorescence measurements were taken on the same leaves used for gas-
296 exchange using a Handy PEA (Hansatech Instruments Ltd., Norfolk, UK). Leaves were dark-
297 adapted for 20-30 min using leaf clips before taking measurements. The saturation pulse rate of
298 3000 µmol m^{-2} s^{-1} was used to measure the emission of chlorophyll fluorescence. The initial
299 chlorophyll fluorescence yield (F_0), the variable chlorophyll fluorescence yield (F_v), and the
300 maximum chlorophyll fluorescence yield (F_m) were recorded. The maximum photochemical
301 efficiency of PSII in dark-adapted leaves was obtained by calculating the ratio of F_v/F_m.

302 **Data availability**

303 All phenotypic data from the QTL and NIL populations are attached to this manuscript as
304 supplemental tables S1-S12 and available via figshare. All marker data was previously used in
305 Khangura *et al.* 2019 and made available to the public via figshare
306 (https://doi.org/10.25387/G3.7370948). All the seed stocks described in this study are available
307 upon request.

308 **Results**

309 **Negative effect of *Oy1-N1989* on time to reproductive maturity is exacerbated by Mo17**

310 While preparing the material for our previous study (Khangura *et al.* 2019), we noticed that *Oy1-*
311 *N1989* exhibited a consistent delay in flowering, as measured by the days to silking and days to
312 pollen anthesis. Heterozygous *Oy1-N1989* mutant plants in the Mo17 × B73 hybrid genetic

313 background flower up to two-weeks later than wild-type siblings (Figure 1; Table S4). The *Oy1-*
314 *N1989* mutants also flower later in an isogenic inbred B73 background; however, the delay is only
315 four days. By contrast, wild-type B73 × Mo17 F_1 hybrid plants flower earlier than the wild-type
316 B73 inbred plants. Maize is protandrous and tassels mature earlier than the ear-inflorescence. The
317 effect of *Oy1-N1989* and flowering time was similar for both anthesis and silk emergence. The
318 window of difference in maturity of the tassel and ear inflorescence, measured as anthesis-silking
319 interval (ASI), is used as an indicator of plant stress in maize (Bolanos and Edmeades 1996). The
320 ASI was wider in the wild-type siblings compared to the mutants in Mo17 × B73 hybrid
321 background (Figure 1G) and not discernably different in the B73 inbred background. Thus, the
322 delay in flowering does not seem to be due to a generic stress effect due to lower chlorophyll
323 contents.

324 **Delayed reproductive maturity of *Oy1-N1989* mutants in B73 × Mo17 mapping populations**
325 **maps to *vey1***

326 If the effect of genetic background on flowering time in *Oy1-N1989* mutants is due to variation in
327 the accumulation of chlorophyll, we expect that the previously described *vey1* QTL from Mo17
328 should make this more severe (Khangura *et al.* 2019). To identify the genetic basis of the flowering
329 time variation in *Oy1-N1989* mutants and test the effect of *vey1*, we recorded flowering time in
330 wild-type and mutant F_1 progenies from the crosses between *Oy1-N1989/+*:B73 pollen-parent with
331 IBM-RILs and Syn10-DH lines. Hereafter, the hybrid populations developed from these crosses
332 will be referred to as the IBM-RILs F_1 and Syn10-DH F_1 populations (Figure 2).

333 Pairwise correlations were calculated between previously reported chlorophyll index
334 measures (Khangura *et al.* 2019) and flowering time traits collected from the same plots (Tables
335 S5 and S6). The chlorophyll index was measured at two time points CCMI (25-30 days after

336 sowing) and CCMII (45-50 days after sowing). In the IBM-RILs crosses, wild-type CCMII
337 displayed a weak but significant negative correlation with wild-type DTA and DTS. Similarly, in
338 the Syn10-DH crosses wild-type CCMI displayed a significant weak negative correlation with
339 wild-type DTA and DTS. This indicates that the phenomena observed in our mutants, reduced
340 chlorophyll content associated with a delay in flowering time was true in the wild-type populations
341 as well, but much less obvious. The variation in chlorophyll content in wild-type plants was not
342 predictive of either mutant CCM or flowering time in the mutants (Figure 3, Table S5, and S6)
343 indicating that the variation in CCM was not under the same control in the mutant and wild-type
344 subpopulations. A dramatic and obvious negative correlation was observed between CCM trait
345 values (CCMI and CCMII) and flowering time in the mutant siblings in both IBM-RILs and
346 Syn10-DH F_1 populations. As was observed in the *Oy1-N1989/+* B73 inbred stock and B73 ×
347 Mo17 hybrids *Oy1-N1989/+* mutants, mutants in these test-cross populations also showed a clear
348 increase in mean values for days to anthesis and silking compared to wild-type siblings (Figure 4).
349 The frequency distribution plot of days to anthesis in mutant siblings of IBM-RILs and
350 Syn10-DH F_1 populations displayed a bimodal distribution, suggesting a single polymorphic locus
351 segregating between B73 and Mo17 was the basis of flowering time variation in *Oy1-N1989*
352 mutants (Figure 5). QTL mapping detected a single QTL on chromosome 10 at similar linkage
353 positions for all mutant derived flowering traits (Figure 5; Tables S7 and S8). This corresponds to
354 the *vey1* locus that we previously described as a major-effect QTL that controls chlorophyll
355 biosynthesis only in the presence of the *Oy1-N1989* allele (Khangura *et al.* 2019). QTL mapping
356 for various direct and derived mutant flowering time traits such as days to flower in the mutant
357 heterozygotes (MT_DTA and MT_DTS), ratio of days to flower derived from mutant and wild-
358 type siblings (Ratio_DTA and Ratio_DTS), and the difference in days to flower between the wild-

359 type and mutant siblings (Diff_DTA and Diff_DTS) all detected *vey1* in both mapping populations
360 and exceeding permutation-estimated significance thresholds (alpha<0.05). The *vey1* QTL
361 explained ~40-48% of the phenotypic variation for these flowering traits in the IBM-RIL crosses,
362 and >65% variation in Syn10-DH F_1 crosses. As expected, the *Oy1-N1989* enhancing $vey1^{Mo17}$
363 allele was associated with a delay in flowering time in the mutant hybrid siblings (Tables S7 and
364 S8). In addition to *vey1*, an additional QTL controlling both mutant anthesis and silking was
365 detected in the Syn10-DH F_1 population on chromosome 2 which we call *other oil yellow1*
366 *flowering time locus1* (*oof1*). This QTL explained ~7-8% variation in flowering time with the
367 Mo17 allele at this locus resulting in a delay of 2-3 days in reproductive maturity of mutant siblings.
368 Because of the very large effect of *vey1*, and the mild segregation distortion at this locus in
369 both bi-parental populations (Khangura *et al.* 2019), weak QTL might be detected by spurious
370 linkage between chr2 and chr10 markers. To test this, we carried out multiple regressions using
371 top markers at *oof1* and *vey1* as independent variables and mutant DTA in the Syn10-DH as a
372 dependent variable (data not shown). In this analysis, both *vey1* and *oof1* remained significant
373 factors in the multiple regression and explained 62% and 2% of the variance in flowering time,
374 respectively. Inclusion of a *vey1* × *oof1* interaction term did not improve the fit of the model, did
375 not eliminate the significance of the *oof1* term, and the interaction term was not a significant
376 variable. Moreover, we did not detect additional QTL by including these as covariates in an
377 additional genome-wide scan. Therefore, we propose that *oof1* is a novel QTL contingent upon the
378 *Oy1-N1989* mutation and genetically independent of *vey1*.
379 The ASI of mutant and wild-type siblings in the test cross populations were not discernably
380 different, just as we observed in the mutant parents. QTL mapping for this trait did not detect any
381 loci controlling ASI in either the mutants or the wild type siblings. In addition, we did not detect

382 any QTL for flowering time in wild-type siblings (Tables S7 and S8). Thus, *Oy1-N1989* was
383 epistatic to both *vey1* and *oof1* QTLs suggesting a role for each locus in controlling either
384 photosynthesis or chlorophyll metabolites in the regulation of flowering time.

385 We further validated the effect of the *vey1* critical region using a set of NIL that vary at the
386 *vey1* QTL from the recurrent background. F_1 progeny of these NIL and *Oy1-N1989*/+ produced
387 matched wild-type and *Oy1-N1989*/+ heterozygous mutant NIL F_1 hybrids. The $vey1^{Mo17}$ allele
388 delayed flowering time in *Oy1-N1989/*+ mutants crossed to both B73 and Mo17 recurrent
389 backgrounds when compared to NILs carrying $vey1^{B73}$ (Figure 6, Figure S3, and Table S3). No
390 effect of *vey1* introgression from either parent was visible on the flowering traits of the wild-type
391 siblings. The reproductive maturity of mutant B73-like NILs carrying $vey1^{Mo17}$, and reciprocal
392 introgression of $vey1^{B73}$ into Mo17 background displayed the opposite effect on flowering time in
393 the F_1 mutants (Figure 6). Thus, these results clearly show the single locus effect of *vey1* on
394 flowering time in maize in *Oy1-N1989*-contingent manner in both isogenic inbred (B73) and
395 hybrid (Mo17 × B73) background.

396 **Expression polymorphism in B73-like NILs is consistent with cis-acting regulatory**
397 **polymorphism at *vey1***

398 Our previous study looking at the suppression of *Oy1-N1989* mutant phenotype using chlorophyll
399 accumulation identified a cis-eQTL at *oy1* in the IBM-RILs population (Khangura *et al.* 2019).
400 Normalized expression (expressed as RPKM) of OY1 derived from 14 days old shoot apices of
401 IBM-RILs (Li et al., 2013; 2018) were used for this analysis. The top marker, isu085b, used in the
402 detection of this cis-eQTL was also one of the top significant markers for mutant flowering time
403 traits (Figure S1 and Table S9). Regression of OY1 expression and flowering traits collected in
404 IBM-RILs F_1 population identified a significant linear relationship between gene expression in

405 wild-type inbred lines and flowering time measurements from mutant F_1 siblings (Figure S2 and
406 Table S9). Roughly 21% of the variation in mutant DTA could be explained by OY1 expression
407 in the IBM-RILs shoot apices. OY1 expression did not predict any variation in wild-type DTA.

408 The allele specific-expression (ASE) assay in our previous study identified bias in expression
409 with the wild-type *oy1* allele from Mo17 displaying lower expression than the wild-type *oy1* allele
410 from B73 (Khangura *et al.* 2019). Our previous ASE work compared mutant plants in two different
411 genetic backgrounds (inbred vs hybrid) which can complicate the interpretations. To overcome
412 this limitation, an ASE assay was designed to test bias at *oy1* using near-isogenic lines in the B73
413 background. These B73-like NILs consisted of two independent NILs with $vey1^{Mo17}$ introgression,
414 and two independent NILs with B73 genotype at *vey1*. Consistent with the previous ASE results,
415 a significantly greater proportion of expression was derived from the *Oy1-N1989* mutant allele
416 when the wild-type *oy1* allele was contributed by $vey1^{Mo17}$ introgression as compared to the
417 isogenic mutant siblings carrying the wild-type *oy1* allele from $vey1^{B73}$ introgression (Table S10).

418 **Net CO_2 assimilation and sugar metabolism is reduced in *Oy1-N1989* mutants in *vey1*-**
419 **dependent manner**

420 We measured net CO_2 assimilation, sub-stomatal CO_2, photosystem II fluorescence, and
421 photosynthate accumulation in enhanced and suppressed *Oy1-N1989/+* mutants. A previous study
422 in maize has shown that reduction in chlorophyll levels in the leaves leads to a reduction in
423 photosynthetic rate (Huang *et al.* 2009). A similar reduction in photosynthetic rate should be
424 displayed by *Oy1-N1989* mutants and the Mo17 allele should show a greater reduction in
425 photosynthesis compared to the B73 allele. We tested this using F_1 progenies derived from the
426 same four B73-like NILs used for the ASE experiment. The negative effect of $vey1^{Mo17}$
427 introgression on chlorophyll accumulation was visible in the *Oy1-N1989* mutant allele background

428 (Figure 6). As expected, photosynthetic rate (A) was reduced in mutants as compared to wild-type
429 siblings, and mutants were modified further by the *vey1* genotype (Table 1). Photosystem II
430 efficiency (Fv/Fm) measurements indicated higher photo-oxidative damage to the photosystem in
431 enhanced mutant plants compared to the suppressed mutants. Wild-type siblings of all four B73-
432 like NIL F_1 progenies showed no statistically significant difference for chlorophyll and gas-
433 exchange measurements. This indicates that, just as for chlorophyll content, the *vey1* QTL affects
434 net CO_2 assimilation in the presence of the *Oy1-N1989* mutant allele. No differences in stomatal
435 conductance (g_s) or transpiration (E) were observed in the mutant plants, however, severe mutant
436 plants showed significantly higher accumulation of intracellular CO_2 (Ci) compared to the
437 suppressed mutants suggesting the failure of the enhanced mutant plants to uptake CO_2 (Table 1).
438 These differences in photosynthetic rate should result in a decrease of non-structural
439 carbohydrate accumulation in the photosynthetic leaf tissue. The levels of non-structural
440 carbohydrates were determined from leaves of the same mutant plants that were used for gas-
441 exchange measurements. Levels of sucrose, glucose, fructose, and starch were measured in these
442 samples. All of these showed a significant reduction in the enhanced mutants compared to the
443 suppressed mutants in the B73 isogenic background (Figure 7 and Table S11). Lower levels of
444 sugars and starch in the *Oy1-N1989/+* mutant heterozygotes enhanced by a *vey1*^{Mo17} allele is
445 consistent with the observation of lower chlorophyll levels and photosynthetic rates in these
446 genotypes compared to the suppressed mutant NILs.

447 **Defoliation of *Zea mays*, *Sorghum bicolor*, and *Setaria viridis* delays reproductive maturity**

448 The existing literature suggests sugars and carbohydrate metabolism play an important role in
449 regulating flowering time in plants (Ohto *et al.* 2001; Seo *et al.* 2011; Wahl *et al.* 2013). We
450 hypothesized that removal of source tissue should mimic the sugar starvation observed in *Oy1-*

451 *N1989* mutants. We used mechanical defoliation to reduce photosynthetic surplus of the plant. The
452 choice of this treatment was intended to deprive plants of leaf area and photosynthate early in
453 development to separate the block in chlorophyll biosynthesis and the loss of photosynthate, which
454 are coupled in the *Oy1-N1989* mutant study. We conducted this experiment using wild-type inbred
455 strains of maize and two other monocot species: *Sorghum bicolor* (sorghum) and *Setaria viridis*
456 (green foxtail). Each species was defoliated at an early vegetative stage when only few leaves had
457 fully expanded. Defoliation delayed flowering in all three species (Figure 8). Maize, sorghum, and
458 green foxtail displayed a delay in flowering by about 13, 7, and 4 days, respectively, compared to
459 the control plants. Remarkably, one-week post-defoliation, newly-emerged leaves displayed a pale
460 leaf color. Chlorophyll estimation using CCM found a reduction in the leaf greenness in the
461 defoliated treatments compared to the control samples (Figure 8). The newly-emerged leaves of
462 defoliated maize, sorghum, and green foxtail showed ~35%, ~48%, and ~58% reduction in CCM,
463 respectively, compared to control plants. Subsequent leaves emerging from the defoliated plants
464 displayed normal leaf color suggesting recovery of the plants from defoliation. We propose that
465 early season defoliation results in the removal of source tissue that might be critical for vegetative
466 to floral transition in grasses but a direct effect of chlorophyll accumulation cannot be ruled out.

467 **Leaf senescence is suppressed by *Oy1-N1989* mutants in a *vey1*-dependent manner**

468 Leaf senescence can be induced in maize by sucrose accumulation in the leaves. This can be
469 accomplished genetically by disrupting sucrose transport (Braun *et al.* 2006; Baker and Braun
470 2008; Slewinski *et al.* 2009) or by preventing the maize ears from acting as a sink (Allison and
471 Weinmann 1970; Sekhon *et al.* 2012, 2019). Previous studies have shown that maize leaf
472 senescence caused by pollination prevention or ear removal before pollination is genotype-
473 dependent (Ceppi et al. 1987). We tested the effect of sugar accumulation in mutant B73-like NILs

474 on induced leaf senescence by pollination prevention. Given the variation in leaf sugar in *Oy1-*
475 *N1989/+* (Figure 7) we expect the mutants exhibit less or later senescence following pollination
476 prevention and modulation of this effect by *vey1*. We observed that 30 days-after-anthesis (DAA),
477 the top leaves of unpollinated wild-type B73 plants showed complete senescence with only a few
478 green patches. Unpollinated *Oy1-N1989/+* F_1 mutant plants crossed to the $vey1^{B73}$ NIL background
479 were green and showed only a few patches of anthocyanin accumulation and cell death on the top
480 leaves at 30 DAA (Figure 9 and Table S12). Consistent with the lower chlorophyll and NSC
481 accumulation, unpollinated *Oy1-N1989/+* mutant F_1 plants crossed to the B73 NIL background
482 containing the $vey1^{Mo17}$ introgression did not show any sign of leaf senescence at 30 DAA. By 42
483 DAA, unpollinated *Oy1-N1989/+* mutants with the $vey1^{B73}$ allele and all unpollinated wild-type
484 plants showed leaf senescence. Even at 42 DAA, the enhancement of *Oy1-N1989/+* by the
485 $vey1^{Mo17}$ allele resulted in substantially less cell death and anthocyanin accumulation.

486 **Discussion**

487 Our previous work identified a modifier, *vey1*, that affects the chlorophyll accumulation in *Oy1-*
488 *N1989/+* heterozygotes (Khangura *et al.* 2019). The *vey1* polymorphism(s) are common natural
489 variant(s) linked to the *oy1* locus of maize. We proposed that *vey1* results from cis-acting
490 regulatory polymorphisms that affect the expression of OY1. The suppression of the mutant, and
491 accumulation of chlorophyll, follows the proportion of wild-type and mutant transcript levels
492 (Table S10 and Khangura *et al.* 2019). In this work, we describe a delay in reproductive maturity
493 in the *Oy1-N1989* mutants and demonstrate that *vey1* encodes a strong modifying QTL altering
494 the flowering time of mutant siblings in all mapping populations (Figures 5 and 6; Tables S7 and
495 S8). Just as the detection of *vey1* for CCM was contingent on the *Oy1-N1989* mutant allele in the

496 background, there was no effect of the *vey1* genotype on flowering time in wild-type siblings. We
497 observed the same marker, isu085b, had the strongest effect on chlorophyll content, OY1 transcript
498 abundance in shoot apices (Khangura *et al.* 2019), and variation in flowering time of IBM-RILs ×
499 *Oy1-N1989/+* mutant F_1 mutant siblings (Table S9 and Figure S2). Taking these observations
500 together, we propose that the cis-acting eQTL at *oy1* is affecting chlorophyll level in *Oy1-N1989*
501 mutants, and that the alteration in photosynthesis through perturbed chlorophyll metabolism
502 affects flowering time variation in mutant siblings in these populations.

503 Our previous work on *vey1* has focused on the cryptic nature of the variation, and the
504 interaction between the *vey1* QTL and the *Oy1-N1989* mutant allele. The experiments presented
505 here also suggest chlorophyll content as a heretofore unappreciated correlate of flowering time in
506 wild-type maize plants (Figure 3; Tables S5 and S6). We observed that CCM values in both test
507 cross populations, were negatively correlated with wild-type days to reproductive maturity. This
508 suggests a role for the determinants of variation in chlorophyll contents in regulation of flowering
509 time in maize perhaps via changes to photosynthetic output or signaling. As no QTL were detected
510 for CCM in the wild-type siblings in our previous work (Khangura *et al.* 2019), it also suggests
511 that the mechanism responsible for the covariation between CCM and flowering time is
512 independent of *vey1*. This is further strengthened by the absence of an effect of *vey1* on flowering
513 time in the wild-type siblings in our mapping populations and NIL experiments (Table S3 and
514 Figure S3). Further experiments are required to validate or reject a causal relationship between
515 CCM and flowering time in wild-type siblings. Experiments using populations with greater
516 recombination or allelic diversity, such as in an association panel, should disrupt most fortuitous
517 linkage and would provide a second test of this phenotypic correlation and either argue for or
518 against additional exploration of this relationship. The crosses of *Oy1-N1989/+* to the association

519 panel analyzed for CCM in a previous study (Khangura *et al.* 2019) could be replanted and
520 measured for flowering time of wild-type and *Oy1-N1989/+* mutant sibling pairs. Candidate gene
521 testing of epistatic interactions between *Oy1-N1989*, *vey1*, and the known flowering time
522 regulators segregating in that population (e.g. *zmmads69*, *cct10*, *zcn8*, *dlf1*, and *vgt1)* could provide
523 some insight. Epistasis, indicating interaction between chlorophyll biosynthetic disruption and
524 developmental determinants of the transition to flowering, would be consistent with
525 photosynthesis acting as part of the autonomous pathway whereas no genetic interaction would be
526 consistent with the slow growth of plant organs in a compromised background resulting in the
527 observed reproductive delays.

528 Even though the Syn10-DH and IBM-RILs are derived from the same parents, they differ in
529 the method of development and rates of recombination (Liu et al. 2015; Hussain et al. 2007; Lee
530 et al. 2002). Thus, these two populations yield different levels of resolution for QTL detection.
531 Our previous analysis to fine map *vey1* QTL using CCM values showed Syn10-DH to have a
532 higher mapping resolution than the IBM-RILs population (Khangura *et al.* 2019). We also
533 observed different QTL for flowering time in these populations. QTL analysis in Syn10-DH F_1
534 population detected the *oof1* QTL on chromosome 2 affecting MT_DTA and MT_DTS as well as
535 the major-effect locus *vey1* (Table S8). The detection of *oof1* was dependent on the presence of
536 the *Oy1-N1989* mutant, but was neither contingent nor displayed any epistatic interactions with
537 *vey1*. Thus, *oof1* appears to be a novel locus of independent mechanism affecting flowering time
538 in the *Oy1-N1989* mutants. This QTL on chromosome 2 was not detected for any other trait in the
539 Syn10-DH and IBM-RILs testcross populations with *Oy1-N1989/+*:B73 in the current study nor
540 was it identified as a modifier of chlorophyll content in our previous study (Khangura *et al.* 2019).
541 The amount of phenotypic variation explained by *vey1* in flowering time was higher in the Syn10-

542 DH experimental material than the IBM-RILs testcross population by ~20% (Tables S7 and S8).
543 Greater variation in flowering time in the IBM-RILs testcross progenies that could not be modeled
544 by marker genotypes may result from higher residual heterozygosity or greater rates of pollen
545 contamination during the single seed descent (SSD) procedure used to generate the IBM-RILs
546 (Lee et al. 2002). Heterozygosity is expected to be negligible in Syn10-DH population because of
547 the DH procedure employed to fix allele segregation during population development (Hussain *et*
548 *al.* 2007). In addition, we had a moderate increase in sample size in the Syn10-DH (251 lines) as
549 compared to the IBM-RILs (216 lines) that is expected to result in a marginally greater power to
550 detect QTL in the Syn10-DH F_1 populations.

551 Chlorophyll levels are correlated with the rate of photosynthesis in plants (Huang *et al.* 2009).
552 Some controversy has been reported in mutants of soybean affected in an ortholog of *oy1* with
553 some reports showing little impact on photosynthesis (Sakowska *et al.* 2018) and others clearly
554 demonstrating a linear relationship between chlorophyll variation and photosynthesis (Walker *et*
555 *al.* 2017). The reasons for conflicting conclusions results from soybean mutants are not fully clear
556 but it warrants some caution in making simplistic interpretations about the impact of chlorophyll
557 deficient mutants on photosynthesis. In our study, net CO_2 assimilation was associated with the
558 severity of the *Oy1-N1989* mutant phenotype. The effect of chlorophyll loss on CO_2 assimilation
559 measurements using a LICOR instrument was somewhat non-linear. A nearly 5-fold reduction in
560 CCM in *Oy1-N1989* NILs carrying a B73 allele at *vey1* resulted in in a 22% reduction in net CO_2
561 assimilation while the 10-fold reduction in CCM in *Oy1-N1989* NILs carrying a Mo17 allele at
562 *vey1* resulted in a 64% reduction in net photosynthetic rate, compared to their isogenic wild-type
563 siblings (Table 1). Ultimately, both reductions resulted in less accumulation of free sugars and

564 starch, with a substantially greater reduction in the enhanced mutant NILs (Figure 7; Tables 1 and
565 S11).

566 The allelic interactions of *Oy1-N1989* and wild-type *oy1* alleles are consistent with the
567 inductive role of carbohydrate status on floral transition (Ohto et al. 2001; Seo et al. 2011; Wahl
568 et al. 2013; Minow et al. 2018). Additional work exploring proposed carbohydrate signaling
569 metabolites, such as T6P and organic acids, and analyses of the downstream floral integrators such
570 as the FT orthologs of maize are still needed to link our results to the existing models of floral
571 transition regulation in maize (Minow *et al.* 2018).

572 One complexity that we observed in our data is that defoliation did not separate
573 photosynthate levels from changes in chlorophyll (Figure 8). The mechanical removal of leaves
574 resulted in changes to CCM in the newly emerging leaves of defoliated plants. As a result, a
575 mechanical treatment served to highlight the interconnected nature of plant metabolism: large
576 changes to any feature of central metabolism or plant physiology results in large changes to all of
577 central metabolism and plant physiology. In an effort to separate photosynthate and chlorophyll
578 accummulation, one can conceive of alternate experiments such as measuring the time to maturity
579 in different light intensities achieved using neutral shade cloth to produce a gradient of
580 photosynthetically active radiation and sugar accumulation. Similarly, plants could be sprayed
581 with low doses of chemicals such as 3-(3,4-dichlorophenyl)-1,1-dimethylurea (DCMU) that
582 disrupt electron transfer during the light reactions to reduce photosynthetic output of plants without
583 altering light fluence experienced by other photoreceptors. However, all these experiments may
584 suffer from the same confounding of NSC and chlorophyll as the defoliation experiment. As a
585 result, researchers should quantify chlorophyll after these treatments as any change in chlorophyll
586 complicate our ability to uncouple chlorophyll metabolism and sugar accumulation as

587 demonstrated by our defoliation experiment and all the carbohydrate partitioning mutants of maize
588 studied to date.

589 Two other subunits of magnesium chelatase are encoded by genes that were identified in
590 Arabidopsis as *genomes uncoupled* mutants, *gun4* and *gun5*, with altered retrograde, plastid-to-
591 nuclear, signaling with defects in chlorophyll metabolism (Susek *et al.* 1993; Mochizuki *et al.*
592 2001; Larkin *et al.* 2003). Multiple studies have demonstrated retrograde signaling mutants with
593 defects in chlorophyll metabolism (Hernández-Verdeja and Strand 2018) and circadian rhythm
594 (Jones 2019). Retrograde signaling events are also associated with cell death, chloroplast
595 development, and etiolation but it acts via a number of modifiers of flowering, including
596 phytochromes, phytochrome signaling components, blue light perception via *crytochrome1,* and
597 circadian rhythmicity of key genes that affect flowering time. While retrograde signaling is an
598 attractive alternative model to sugar signaling for the phenomena reported here, mutants in
599 orthologs of *oy1* in both monocots and dicots (Mochizuki *et al.* 2001; Gadjieva *et al.* 2005) have
600 been tested for a *genomes uncoupled* phenotype and they did not perturb retrograde signaling. This
601 makes it unlikely that *Oy1-N1989* and *vey1* are altering flowering time via aberrant retrograde
602 signals. Additional experiments are necessary to clearly separate the effects of chlorophyll
603 metabolite levels from photosynthate levels to independently test their effects on flowering time
604 in maize.

605 We have known that defoliation is practiced in some maize nurseries to stagger flowering
606 time and permit intercrossing of lines with divergent reproductive maturities. We had presumed
607 that this was based on published research. Remarkably, we were not able to find a reference for
608 this practice. Previous work on defoliation in maize has looked at the effect of early and late season
609 defoliation on growth, and yield components but did not report flowering times (Crookston and

610 Hicks 1988; Pearson and Fletcher 2009). As a result, Figure 8 provides information that was
611 informally shared within the maize genetics research community but not described formally. In
612 addition, we extended this observation from maize to both sorghum and green foxtail, indicating
613 that defoliation can achieve staggered flowering times in these species as well. This may be a
614 general feature of grasses, but appears to not be universal in angiosperms as early-season
615 defoliation of photoperiod-sensitive strawberries did not affect flowering time (Guttridge 1959).

616 Sugar export and phloem loading mutants in maize that carry lesions in *tie-dyed1*, *tie-dyed2*,
617 *sucrose export defective1*, *psychedelic*, and *sucrose trasporter1* have all been shown to delay
618 flowering time (Braun *et al.* 2006; Baker and Braun 2008; Ma *et al.* 2008; Slewinski *et al.* 2009;
619 Slewinski and Braun 2010). We also observed declines in sugar levels in *Oy1-N1989* mutants
620 (Figure 7 and Table S11) and a delay in flowering time (Figure 1). It is tempting to consider these
621 mutants as a demonstration that sugar signaling can work independent of chlorophyll, but these
622 mutants also display low chlorophyll contents (Braun *et al.* 2006; Baker and Braun 2008; Ma *et*
623 *al.* 2008; Slewinski *et al.* 2009; Slewinski and Braun 2010). Curiously, *sucrose export defective1*
624 encodes tocopherol cyclase (Porfirova *et al.* 2002; Sattler *et al.* 2003). Tocopherol and chlorophyll
625 share the phytol side chain, and the salvage pathway for phytol side chains from chlorophyll can
626 contribute to tocopherol accumulation in both maize and Arabidopsis (Ischebeck *et al.* 2006;
627 Schelbert *et al.* 2009; Diepenbrock *et al.* 2017). While it is attractive to try and unify these findings,
628 chlorophyll breakdown products were only rate limiting for tocopherol synthesis in senescent
629 tissues of Arabidopsis (Zhang *et al.* 2014). Furthermore, in *Oy1-N1989* mutants the phytol
630 precursors should be abundant as this pool is not being consumed by chlorophyll biosynthesis.
631 Future experiments that more carefully explore these metabolites, for instance, via other mutants

632 that do not simultaneously affect multiple pathways, especially chlorophyll metabolism, are
633 required.

634 Accumulation of sugars in the leaves due to sink disruption has been proposed to induce leaf
635 senescence in a variety of angiosperms, including maize and Arabidopsis (Allison and Weinmann
636 1970; Ceppi *et al.* 1987; Pourtau *et al.* 2006; Sekhon *et al.* 2012, 2019). In maize, leaf senescence
637 is triggered when pollination is prevented and sucrose accumulates in leaves due to the lack of the
638 sink activity of a pollinated ear (Allison and Weinmann 1970; Ceppi *et al.* 1987). This sucrose-
639 dependent leaf senescence is genotype-dependent, and B73 is particularly susceptible to this
640 phenomenon. Genetic inheritance of the induced senescence phenomenon in maize inbred line
641 B73 was proposed to be under the control of a single dominant locus (Ceppi *et al.* 1987). The leaf
642 senescent phenotypes of the sucrose export mutants demonstrate that excessive photosynthate
643 accumulation can cause tissue to senesce regardless of ear presence (Braun *et al.* 2006; Baker and
644 Braun 2008; Ma *et al.* 2008; Slewinski *et al.* 2009). Induced leaf senescence by sink removal or
645 sugar application shows some overlap of biochemical and molecular mechanisms with natural
646 senescence in plants (summarized in Sekhon *et al*. 2012). A study of gene expression in the B73
647 inbred of maize identified senescence associated genes that exhibit gene expression changes during
648 pollination-prevented leaf senescence (Sekhon *et al*. 2012). We found that leaf senescence could
649 be prevented or delayed by the suppression of photosynthesis in the *Oy1-N1989* mutant and further
650 modulated by *vey1* variants (Figure 9 and Table S12). We expect that future gene expression
651 studies in *Oy1-N1989* mutant and sugar export mutants will identify genes consistently impacted
652 by lower and higher chlorophyll levels, presumably including senescence associated genes and
653 genes regulating carbohydrate metabolism.

Acknowledgements

We would like to thank the National Science Foundation for NSF grant 1444503 awarded to G.S.J. and B.P.D which helped fund this research. We thank the Purdue ACRE and ICSC staff members Mr. Jim Beaty and Mr. Jason Adams for help with planting, and management of the field experiments described in this work. We also thank past Johal lab members for help with planting and data collection. We would like to thank Mr. Mike Gosney for helping with gas-exchange measurements. We gratefully acknowledge solidarity with the the operator of the compact track loader who provided a soundtrack and dry workspace by excavating and constructing a French drain on our office walls while we wrote this paper.

664 **REFERENCES**

665 Abe, M., Y. Kobayashi, S. Yamamoto, Y. Daimon, A. Yamaguchi *et al.*, 2005 FD , a bZIP Protein
666 Mediating Signals from the Floral Pathway Integrator FT at the Shoot Apex. Science 309:
667 1052–1056.

668 Allison, J. C. S., and H. Weinmann, 1970 Effect of absence of developing grain on carbohydrate
669 content and senescence of maize leaves. Plant Physiol. 46: 435–436.

670 Alter, P., S. Bircheneder, L.-Z. Zhou, U. Schlüter, M. Gahrtz *et al.*, 2016 Flowering Time-
671 Regulated Genes in Maize Include the Transcription Factor ZmMADS1. Plant Physiol. 172:
672 389–404.

673 Amasino, R. M., and S. D. Michaels, 2010 The Timing of Flowering. Plant Physiol. 154: 516–520.

674 Baker, R. F., and D. M. Braun, 2008 Tie-dyed2 functions with tie-dyed1 to promote carbohydrate
675 export from maize leaves. Plant Physiol. 146: 1085–1097.

676 Bolanos, J., and G. O. Edmeades, 1996 The importance of the anthesis-silking interval in breeding
677 for drought tolerance in tropical maize. F. Crop. Res. 48: 65–80.

678 Bouchet, S., P. Bertin, T. Presterl, P. Jamin, D. Coubriche *et al.*, 2017 Association mapping for
679 phenology and plant architecture in maize shows higher power for developmental traits
680 compared with growth influenced traits. Heredity (Edinb). 118: 249–259.

681 Braun, D. M., Y. Ma, N. Inada, M. G. Muszynski, and R. F. Baker, 2006 tie-dyed1 Regulates
682 carbohydrate accumulation in maize leaves. Plant Physiol. 142: 1511–22.

683 Broman, K. W., H. Wu, S. Sen, and G. a. Churchill, 2003 R/qtl: QTL mapping in experimental
684 crosses. Bioinformatics 19: 889–890.

685 Buckler, E. S., J. B. Holland, P. J. Bradbury, C. B. Acharya, P. J. Brown *et al.*, 2009 The genetic
686 architecture of maize flowering time. Science 325: 714–718.

687 Ceppi, D., M. Sala, E. Gentinetta, A. Verderio, and M. Motto, 1987 Genotype-Dependent Leaf
688 Senescence in Maize: Inheritance and effects of pollination-prevention. Plant Physiol. 85:
689 720–725.

690 Chen, M., J. Chory, and C. Fankhauser, 2004 Light Signal Transduction in Higher Plants. Annu.
691 Rev. Genet. 38: 87–117.

692 Cho, L. H., R. Pasriga, J. Yoon, J. S. Jeon, and G. An, 2018 Roles of Sugars in Controlling
693 Flowering Time. J. Plant Biol. 61: 121–130.

694 Cho, L. H., J. Yoon, and G. An, 2017 The control of flowering time by environmental factors.
695 Plant J. 90: 708–719.

696 Colasanti, J., Z. Yuan, and V. Sundaresan, 1998 The indeterminate gene encodes a zinc finger
697 protein and regulates a leaf-generated signal required for thetransition to flowering in maize.
698 Cell 93: 593–603.

699 Coles, N. D., M. D. McMullen, P. J. Balint-Kurti, R. C. Pratt, and J. B. Holland, 2010 Genetic
700 control of photoperiod sensitivity in maize revealed by joint multiple population analysis.

701 Genetics 184: 799–812.

702 Coneva, V., D. Guevara, S. J. Rothstein, and J. Colasanti, 2012 Transcript and metabolite signature
703 of maize source leaves suggests a link between transitory starch to sucrose balance and the
704 autonomous floral transition. J. Exp. Bot. 63: 5079–5092.

705 Coneva, V., T. Zhu, and J. Colasanti, 2007 Expression differences between normal and
706 indeterminate1 maize suggest downstream targets of ID1, a floral transition regulator in maize.
707 J. Exp. Bot. 58: 3679–3693.

708 Corbesier, L., P. Lejeune, and G. Bernier, 1998 The role of carbohydrates in the induction of
709 flowering in Arabidopsis thaliana: Comparison between the wild type and a starchless mutant.
710 Planta 206: 131–137.

711 Corbesier, L., C. Vincent, S. Jang, F. Fornara, Q. Fan *et al.*, 2007 FT protein movement contributes
712 to long-distance signaling in floral induction of Arabidopsis. Science 316: 1030–1033.

713 Crookston, R. K., and D. R. Hicks, 1988 Effect of Early Defoliation on Maize Growth and Yield:
714 an Eleven-year Perspective. Crop Sci. 28: 371–373.

715 Danilevskaya, O. N., X. Meng, D. A. Selinger, S. Deschamps, P. Hermon *et al.*, 2008 Involvement
716 of the MADS-Box Gene ZMM4 in Floral Induction and Inflorescence Development in Maize.
717 Plant Physiol. 147: 2054–2069.

718 DePristo, M. A., E. Banks, R. Poplin, K. V Garimella, J. R. Maguire *et al.*, 2011 A framework for
719 variation discovery and genotyping using next-generation DNA sequencing data. Nat. Genet.
720 43: 491–498.

721 Diepenbrock, C. H., C. B. Kandianis, A. E. Lipka, M. Magallanes-Lundback, B. Vaillancourt *et*
722 *al.*, 2017 Novel Loci Underlie Natural Variation in Vitamin E Levels in Maize Grain. Plant
723 Cell 29: 2374–2392.

724 Doebley, J., A. Stec, and L. Hubbard, 1997 The evolution of apical dominance in maize. Nature
725 386: 485–488.

726 Eichten, S. R., J. M. Foerster, N. de Leon, Y. Kai, C.-T. Yeh *et al.*, 2011 B73-Mo17 near-isogenic
727 lines demonstrate dispersed structural variation in maize. Plant Physiol. 156: 1679–90.

728 Evans, M. M., and R. S. Poethig, 1995 Gibberellins promote vegetative phase change and
729 reproductive maturity in maize. Plant Physiol. 108: 475–87.

730 Eveland, A. L., and D. P. Jackson, 2012 Sugars, signalling, and plant development. J. Exp. Bot.
731 63: 3367–3377.

732 Gadjieva, R., E. Axelsson, U. Olsson, and M. Hansson, 2005 Analysis of gun phenotype in barley
733 magnesium chelatase and Mg-protoporphyrin IX monomethyl ester cyclase mutants. Plant
734 Physiol. Biochem. 43: 901–908.

735 Gibson, L. C. D., R. D. Willows, C. G. Kannangara, D. von Wettstein, and C. N. Hunter, 1995
736 Magnesium-protoporphyrin chelatase of Rhodobacter sphaeroides: reconstitution of activity
737 by combining the products of the bchH, -I, and -D genes expressed in Escherichia coli. Proc.
738 Natl. Acad. Sci. U. S. A. 92: 1941–1944.

739 Guo, L., X. Wang, M. Zhao, C. Huang, C. Li *et al.*, 2018 Stepwise cis-Regulatory Changes in
740 ZCN8 Contribute to Maize Flowering-Time Adaptation. Curr. Biol. 28: 3005–3015.e4.

741 Guttridge, C. G., 1959 Evidence for a Flower Inhibitor and Vegetative Growth Promoter in the
742 Strawberry. Ann. Bot. 23: 351–360.

743 Hansson, A., C. G. Kannangara, D. V Wettstein, and M. Hansson, 1999 Molecular basis for
744 semidominance of missense mutations in the XANTHA-H (42-kDa) subunit of magnesium
745 chelatase. Proc. Natl. Acad. Sci. U. S. A. 96: 1744–1749.

746 Hansson, A., R. D. Willows, T. H. Roberts, and M. Hansson, 2002 Three semidominant barley
747 mutants with single amino acid substitutions in the smallest magnesium chelatase subunit
748 form defective AAA+ hexamers. Proc. Natl. Acad. Sci. U. S. A. 99: 13944–13949.

749 Hernández-Verdeja, T., and Å. Strand, 2018 Retrograde Signals Navigate the Path to Chloroplast
750 Development. Plant Physiol. 176: 967–976.

751 Huang, M., T. L. Slewinski, R. F. Baker, D. Janick-Buckner, B. Buckner *et al.*, 2009 Camouflage
752 patterning in maize leaves results from a defect in porphobilinogen deaminase. Mol. Plant 2:
753 773–89.

754 Huang, C., H. Sun, D. Xu, Q. Chen, Y. Liang *et al.*, 2017 ZmCCT9 enhances maize adaptation to
755 higher latitudes. Proc. Natl. Acad. Sci. 115: E334–E341.

756 Hung, H.-Y., L. M. Shannon, F. Tian, P. J. Bradbury, C. Chen *et al.*, 2012 ZmCCT and the genetic
757 basis of day-length adaptation underlying the postdomestication spread of maize. Proc. Natl.
758 Acad. Sci. 109: E1913–E1921.

759 Hussain, T., P. Tausend, G. Graham, and J. Ho, 2007 Registration of IBM2 SYN10 Doubled
760 Haploid Mapping Population of Maize. J. Plant Regist. 1: 81.

761 Ischebeck, T., A. M. Zbierzak, M. Kanwischer, and P. Dörmann, 2006 A salvage pathway for
762 phytol metabolism in Arabidopsis. J. Biol. Chem. 281: 2470–2477.

763 Jones, M. A., 2019 Retrograde signalling as an informant of circadian timing. New Phytol. 221:
764 1749–1753.

765 Khangura, R. S., S. Marla, B. P. Venkata, N. J. Heller, G. S. Johal *et al.*, 2019 A Very Oil Yellow1
766 Modifier of the Oil Yellow1-N1989 Allele Uncovers a Cryptic Phenotypic Impact of Cis-
767 regulatory Variation in Maize. G3 9: 375–390.

768 Kozaki, A., S. Hake, and J. Colasanti, 2004 The maize ID1 flowering time regulator is a zinc finger
769 protein with novel DNA binding properties. Nucleic Acids Res. 32: 1710–1720.

770 Lang, A., 1952 Physiology of Flowering. Ann. Rev. Plant. Physiol. 3: 265–306.

771 Lang, A., 1957 The effect of gibberellin upon flower formation. Proc. Natl. Acad. Sci. 43: 709–
772 717.

773 Larkin, R. M., J. M. Alonso, J. R. Ecker, and J. Chory, 2003 GUN4, a regulator of chlorophyll
774 synthesis and intracellular signaling. Science 299: 902–906.

775 Leach, K. A., and D. M. Braun, 2016 Soluble Sugar and Starch Extraction and Quantification from
776 Maize (*Zea mays*) Leaves. Curr. Protoc. Plant Biol. 1: 139–161.

777 Leach, K. A., T. M. Tran, T. L. Slewinski, R. B. Meeley, and D. M. Braun, 2017 Sucrose
778 transporter2 contributes to maize growth, development, and crop yield. J. Integr. Plant Biol.
779 59: 390–408.

780 Lee, M., N. Sharopova, W. D. Beavis, D. Grant, M. Katt *et al.*, 2002 Expanding the genetic map
781 of maize with the intermated B73 x Mo17 (IBM) population. Plant Mol. Biol. 48: 453–61.

782 Liang, Y., Q. Liu, X. Wang, C. Huang, G. Xu *et al.*, 2019 ZmMADS69 functions as a flowering
783 activator through the ZmRap2.7-ZCN8 regulatory module and contributes to maize flowering
784 time adaptation. New Phytol. 221: 2335–2347.

785 Liu, H., Y. Niu, P. J. Gonzalez-Portilla, H. Zhou, L. Wang *et al.*, 2015 An ultra-high-density map
786 as a community resource for discerning the genetic basis of quantitative traits in maize. BMC
787 Genomics 16: 1078.

788 Ma, Y., R. F. Baker, M. Magallanes-Lundback, D. Dellapenna, and D. M. Braun, 2008 Tie-dyed1
789 and Sucrose export defective1 act independently to promote carbohydrate export from maize
790 leaves. Planta 227: 527–538.

791 Meng, X., M. G. Muszynski, and O. N. Danilevskaya, 2011 The FT-Like ZCN8 Gene Functions
792 as a Floral Activator and Is Involved in Photoperiod Sensitivity in Maize. Plant Cell 23: 942–
793 960.

794 Minow, M. A. A., L. M. Ávila, K. Turner, E. Ponzoni, I. Mascheretti *et al.*, 2018 Distinct gene
795 networks modulate floral induction of autonomous maize and photoperiod-dependent teosinte.
796 J. Exp. Bot. 69: 2937–2952.

797 Mochizuki, N., J. a Brusslan, R. Larkin, a Nagatani, and J. Chory, 2001 Arabidopsis genomes
798 uncoupled 5 (GUN5) mutant reveals the involvement of Mg-chelatase H subunit in plastid-
799 to-nucleus signal transduction. Proc. Natl. Acad. Sci. U. S. A. 98: 2053–2058.

800 Moghaddam, M. R. B., and W. Van den Ende, 2013 Sugars, the clock and transition to flowering.
801 Front. Plant Sci. 4: 1–6.

802 Muszynski, M. G., T. Dam, B. Li, D. M. Shirbroun, Z. Hou *et al.*, 2006 delayed flowering1
803 Encodes a basic leucine zipper protein that mediates floral inductive signals at the shoot apex
804 in maize. Plant Physiol. 142: 1523–1536.

805 Mutasa-Göttgens, E., and P. Hedden, 2009 Gibberellin as a factor in floral regulatory networks. J.
806 Exp. Bot. 60: 1979–1989.

807 Ohto, M.-A., K. Onai, Y. Furukawa, E. Aoki, T. Araki *et al.*, 2001 Effects of Sugar on Vegetative
808 Development and Floral Transition in Arabidopsis. Plant Physiol. 127: 252–261.

809 Paul, M. J., 2008 Trehalose 6-phosphate: a signal of sucrose status. Biochem. J. 412: 1–2.

810 Pearson, A., and A. L. Fletcher, 2009 Effect of total defoliation on maize growth and yield. Agron.
811 New Zeal. 39: 1–6.

812 Porfirova, S., E. Bergmuller, S. Tropf, R. Lemke, and P. Dormann, 2002 Isolation of an
813 Arabidopsis mutant lacking vitamin E and identification of a cyclase essential for all
814 tocopherol biosynthesis. Proc. Natl. Acad. Sci. 99: 12495–12500.

815 Pourtau, N., R. Jennings, E. Pelzer, J. Pallas, and A. Wingler, 2006 Effect of sugar-induced
816 senescence on gene expression and implications for the regulation of senescence in
817 Arabidopsis. Planta 224: 556–568.

818 R core Team, 2013 R: A language and environment for statistical computing. R Foundation for
819 Statistical Computing, Vienna, Austria. ISBN 3-900051-07-0, http://www.R-project.org/.

820 Sakowska, K., G. Alberti, L. Genesio, A. Peressotti, G. Delle Vedove *et al.*, 2018 Leaf and canopy
821 photosynthesis of a chlorophyll deficient soybean mutant. Plant Cell Environ. 41: 1427–1437.

822 Salvi, S., G. Sponza, M. Morgante, D. Tomes, X. Niu *et al.*, 2007 Conserved noncoding genomic
823 sequences associated with a flowering-time quantitative trait locus in maize. Proc. Natl. Acad.
824 Sci. U. S. A. 104: 11376–11381.

825 Samach, A., H. Onouchi, S. E. Gold, G. S. Ditta, Z. Schwarz- *et al.*, 2000 Distinct Roles of
826 CONSTANS Target Genes in Reproductive Development of Arabidopsis. Science 288:
827 1613–1616.

828 Sattler, S. E., E. B. Cahoon, S. J. Coughlan, and D. Dellapenna, 2003 Characterization of
829 Tocopherol Cyclases from Higher Plants and Cyanobacteria . Evolutionary Implications for
830 Tocopherol Synthesis and Function. Plant Physiol. 132: 2184–2195.

831 Sawers, R. J. H., J. Viney, P. R. Farmer, R. R. Bussey, G. Olsefski *et al.*, 2006 The maize Oil
832 yellow1 (Oy1) gene encodes the I subunit of magnesium chelatase. Plant Mol. Biol. 60: 95–
833 106.

834 Schelbert, S., S. Aubry, B. Burla, B. Agne, F. Kessler *et al.*, 2009 Pheophytin Pheophorbide
835 Hydrolase (Pheophytinase) Is Involved in Chlorophyll Breakdown during Leaf Senescence
836 in Arabidopsis. Plant Cell 21: 767–785.

837 Searle, N. E., 1965 Physiology of Flowering. Ann. Rev. Plant. Physiol. 16: 97–118.

838 Sekhon, R. S., K. L. Childs, N. Santoro, C. E. Foster, C. R. Buell *et al.*, 2012 Transcriptional and
839 Metabolic Analysis of Senescence Induced by Preventing Pollination in Maize. Plant Physiol.
840 159: 1730–1744.

841 Sekhon, R. S., C. Saski, R. Kumar, B. Flinn, F. Luo *et al.*, 2019 Integrated Genome-Scale Analysis
842 Identifies Novel Genes and Networks Underlying Senescence in Maize. Plant Cell
843 tpc.00930.2018.

844 Sen, T. Z., L. C. Harper, M. L. Schaeffer, C. M. Andorf, T. E. Seigfried *et al.*, 2010 Choosing a
845 genome browser for a Model Organism Database: surveying the Maize community. Database
846 2010: 1–9.

847 Seo, P. J., J. Ryu, S. K. Kang, and C. M. Park, 2011 Modulation of sugar metabolism by an
848 INDETERMINATE DOMAIN transcription factor contributes to photoperiodic flowering in
849 Arabidopsis. Plant J. 65: 418–429.

850 Slewinski, T. L., and D. M. Braun, 2010 The Psychedelic genes of maize redundantly promote
851 carbohydrate export from leaves. Genetics 185: 221–232.

852 Slewinski, T. L., A. Garg, G. S. Johal, and D. M. Braun, 2010 Maize SUT1 functions in phloem
853 loading. Plant Signal. Behav. 5: 1–4.

854 Slewinski, T. L., R. Meeley, and D. M. Braun, 2009 Sucrose transporter1 functions in phloem
855 loading in maize leaves. J. Exp. Bot. 60: 881–892.

856 Steinhoff, J., W. Liu, J. C. Reif, G. Della Porta, N. Ranc *et al.*, 2012 Detection of QTL for
857 flowering time in multiple families of elite maize. Theor. Appl. Genet. 125:.

858 Susek, R. E., F. M. Ausubel, and J. Chory, 1993 Signal Transduction Mutants of Arabidopsis
859 Uncouple Nuclear CAB and RBCS Gene Expression from Chloroplast Development. Cell 74:

860 787–799.

861 Swarts, K., R. M. Gutaker, B. Benz, M. Blake, R. Bukowski *et al.*, 2017 Genomic estimation of
862 complex traits reveals ancient maize adaptation to temperate North America. Science 357:
863 512–515.

864 Vega, S. H., M. Sauer, J. A. J. Orkwiszewski, and S. Poethig, 2002 The early phase change gene
865 in Maize. Plant Cell 14: 133–147.

866 Wahl, V., J. Ponnu, A. Schlereth, S. Arrivault, T. Langenecker *et al.*, 2013 Regulation of flowering
867 by Trehalose-6-phosphate signalling in Arabidopsis thaliana. Science 339: 704–708.

868 Walker, B. J., D. T. Drewry, R. A. Slattery, A. VanLoocke, Y. B. Cho *et al.*, 2017 Chlorophyll can
869 be reduced in crop canopies with little penalty to photosynthesis. Plant Physiol. 176: 1215–
870 1232.

871 Walker, C. J., and J. D. Weinstein, 1991 In vitro assay of the chlorophyll biosynthetic enzyme Mg-
872 chelatase: resolution of the activity into soluble and membrane-bound fractions. Proc. Natl.
873 Acad. Sci. U. S. A. 88: 5789–5793.

874 Wang, R. L., A. Stec, J. Hey, L. Lukens, and J. Doebley, 1999 The limits of selection during maize
875 domestication. Nature 398: 236–239.

876 Wigge, P. A., M. C. Kim, K. E. Jaeger, W. Busch, M. Schmid *et al.*, 2005 Integration of Spatial
877 and Temporal Information During Floral Induction in Arabidopsis. Science 309: 1056–1059.

878 Yoo, S. K., K. S. Chung, J. Kim, J. H. Lee, S. M. Hong *et al.*, 2005 CONSTANS Activates
879 SUPPRESSOR OF OVEREXPRESSION OF CONSTANS 1 through FLOWERING
880 LOCUS T to Promote Flowering in Arabidopsis. Plant Physiol. 139: 770–778.

881 Zeevaart, J. A. D., 1962 Physiology of Flowering. Science 137: 723–731.

882 Zhang, W., T. Liu, G. Ren, S. Hörtensteiner, Y. Zhou *et al.*, 2014 Chlorophyll Degradation: The
883 Tocopherol Biosynthesis-Related Phytol Hydrolase in Arabidopsis Seeds Is Still Missing.
884 Plant Physiol. 166: 70–79.

885 Zhang, L., H. Yu, S. Lin, and Y. Gao, 2016 Molecular Characterization of FT and FD Homologs
886 from Eriobotrya deflexa Nakai forma koshunensis. Front. Plant Sci. 7: 1–10.

887

Table 1. The chlorophyll index, gas-exchange, and maximum quantum yield of the mutant (*Oy1-N1989/+*) and wild-type (+/+) siblings in four independent B73-like NILs x *Oy1-N1989/+*:B73 F_1 progenies.

Genotype[1]	*vey1*-status	CCM[1]	A[2]	g_s[3]	C_i[4]	E[5]	F_v/F_m[6]
Oy1-N1989/+:b094	$vey1^{Mo17}$	1.5±0.04[a]	4.9±1.55[a]	0.2±0.07	331.3±5.01[a]	4.3±0.99	0.16±0.03[a]
Oy1-N1989/+:b189	$vey1^{Mo17}$	1.6±0.14[a]	6.3±0.85[a]	0.2±0.06	319.9±24.93[a]	4.7±0.92	0.16±0.04[a]
Oy1-N1989/+:b135	$vey1^{B73}$	4.9±0.27[b]	27.9±2.47[b]	0.3±0.01	172.4±13.36[b]	5.8±0.49	0.43±0.01[b]
Oy1-N1989/+:b185	$vey1^{B73}$	4.4±0.29[b]	23.5±1.66[b]	0.3±0.03	202.1±27.97[b]	5.5±0.26	0.42±0.02[b]
+/+:b094	$vey1^{Mo17}$	19.7±3.14	34.4±3.97	0.4±0.12	176.1±25.61	6.9±0.84	0.66±0.04
+/+:b189	$vey1^{Mo17}$	14.4±0.66	27.8±0.91	0.3±0.03	166.4±7.39	5.5±0.41	0.70±0.05
+/+:b135	$vey1^{B73}$	19.2±3.47	32.6±3.32	0.3±0.05	162.0±13.11	6.4±0.52	0.72±0.03
+/+:b185	$vey1^{B73}$	22.4±1.84	33.2±2.49	0.4±0.06	166.6±13.76	6.5±0.53	0.72±0.03

The data are provided as mean ± standard deviations of three experimental replications. Each replication consisted of three independent plants measurements for mutants and two for wild-type siblings. The superscript connecting letter report between each genotype group (mutant or wild-type) indicates statistical significance determined using ANOVA with post-hoc analysis using Tukey's HSD at $p<0.01$. No statistically significant difference was found between the wild-type siblings.

[1]Chlorophyll index measured using CCM-200 plus; [2]Net CO_2 assimilation rate (µmol CO_2 m^{-2} s^{-1}); [3]Stomatal conductance (mol H_2O m^{-2} s^{-1}); [4]Substomatal CO_2 concentration (µmol CO_2 mol air^{-1}); [5]Transpiration rate (mmol m^{-2} s^{-1}); [6]Maximum quantum yield of PSII (Fv/Fm)

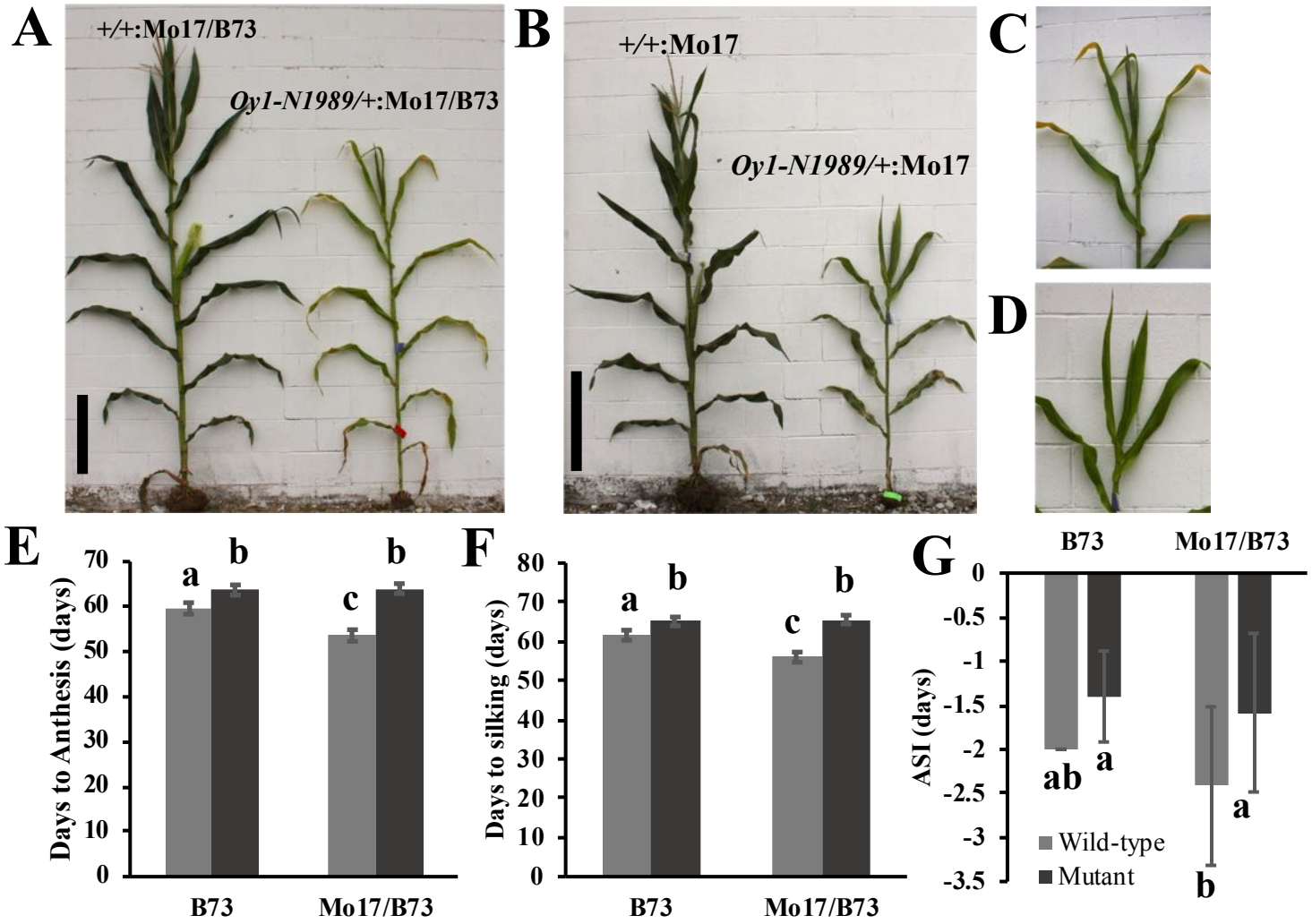

Figure 1. The reproductive maturity is delayed by *Oy1-N1989* allele in maize. The representative (A) wild-type (left) and mutant (right) sibling from Mo17 x *Oy1-N1989/+*:B73 cross (reproduced from Figure 1b in Khangura *et. al*. 2019), black scale bar = 50 cm. The representative (B) wild-type (left) and mutant (right) sibling from Mo17 x *Oy1-N1989/+*:Mo17 cross (BC_7). The close-up view of the emerging tassel of mutant siblings (C) in panel A, and (D) panel B. The distribution of (E) days to anthesis, (F) days to silking, and (G) anthesis-silking interval (ASI) in the wild-type and mutant siblings in B73 and Mo17 x B73 (Mo17/B73) hybrid genetic backgrounds.

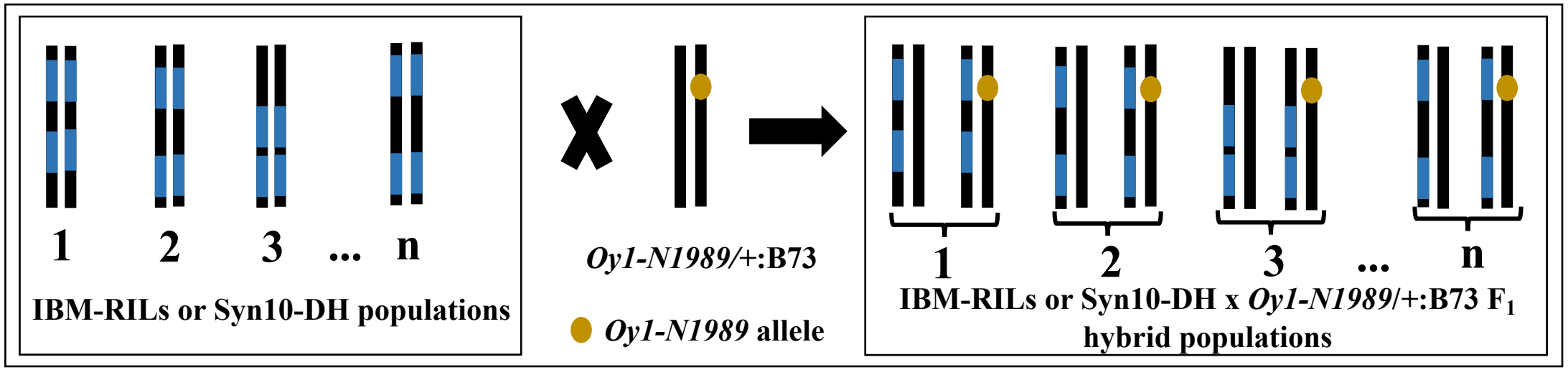

Figure 2. The schematic of crossing strategy used to map *Oy1-N1989* enhancer/suppressor loci using IBM-RILs (n=216) and Syn10-DH (n=251) populations. Black and blue colors indicate B73 and Mo17 genotypes. Chromosome 10 of the heterozygous pollen-parent *Oy1-N1989/+*:B73 is shown with a golden spot indicating *Oy1-N1989* mutant allele. The resulting F_1 progenies from these crosses are depicted with state of chromosome 10 for each F_1 testcross showing segregation of wild-type and mutant (with the golden spot) siblings.

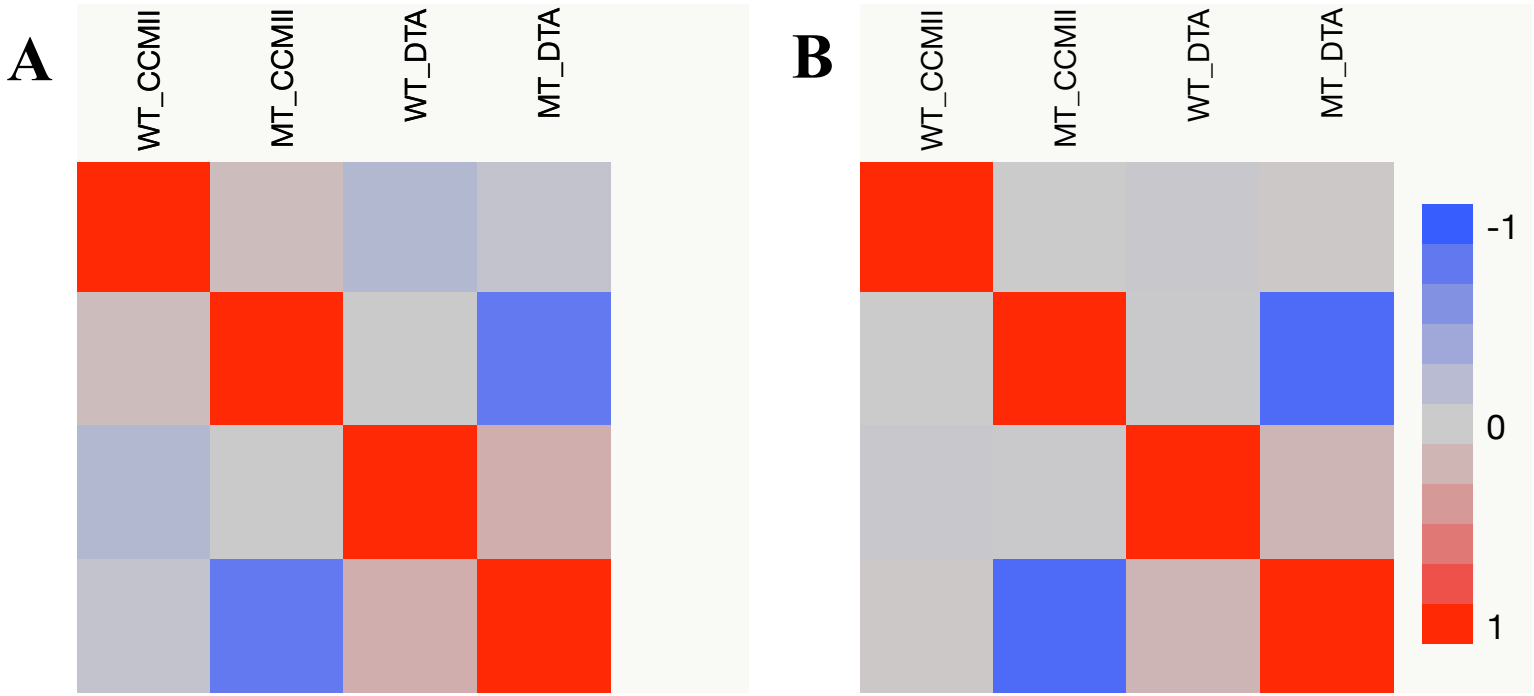

Figure 3. The pairwise correlation matrix showing color-coded correlation values between wild-type CCMII (WT_CCMII), mutant CCMII (MT_CCMII), wild-type days to anthesis (WT_DTA), and mutant days to anthesis (MT_DTA) in (A) IBM-RILs x *Oy1-N1989/+*:B73, and (B) Syn10-DH x *Oy1-N1989/+*:B73 F_1 test cross populations.

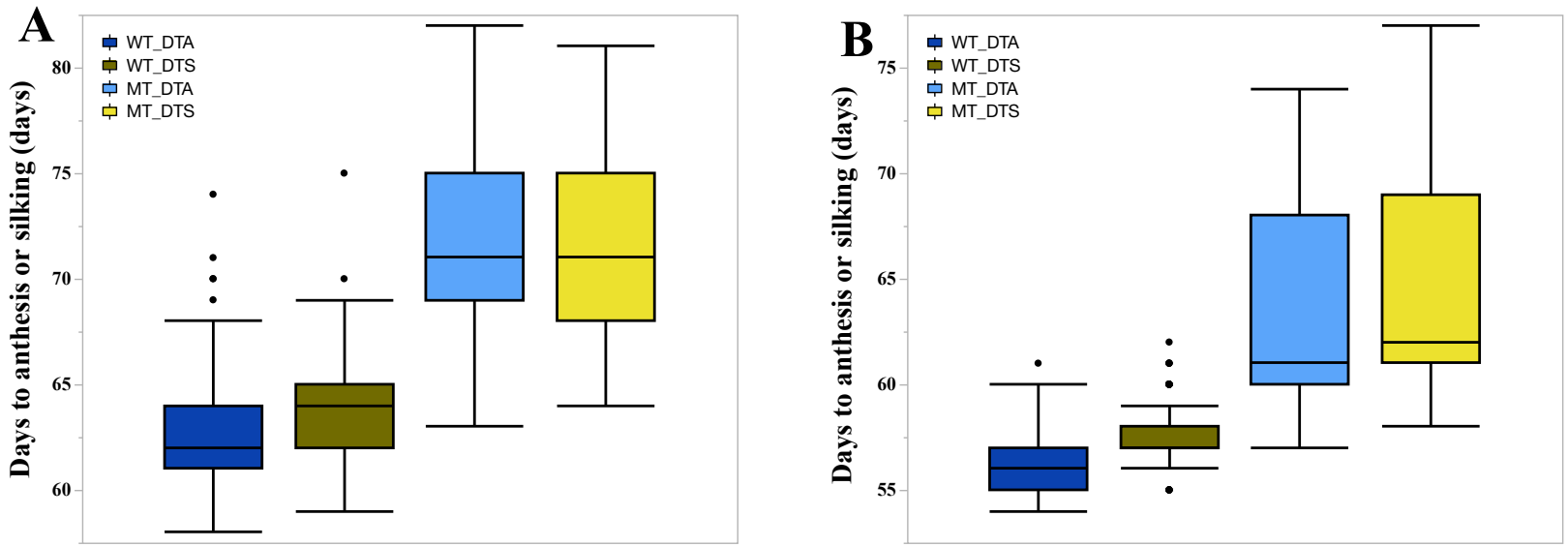

Figure 4. The distribution of days to flower (anthesis and silking) in the wild-type and mutant siblings in (A) IBM-RILs x *Oy1-N1989/+*:B73, and (B) Syn10-DH x *Oy1-N1989/+*:B73 F_1 test cross populations. Abbreviations: wild-type days to anthesis (WT_DTA), wild-type days to silking (WT_DTS), mutant days to anthesis (MT_DTA), and mutant days to silking (DTS).

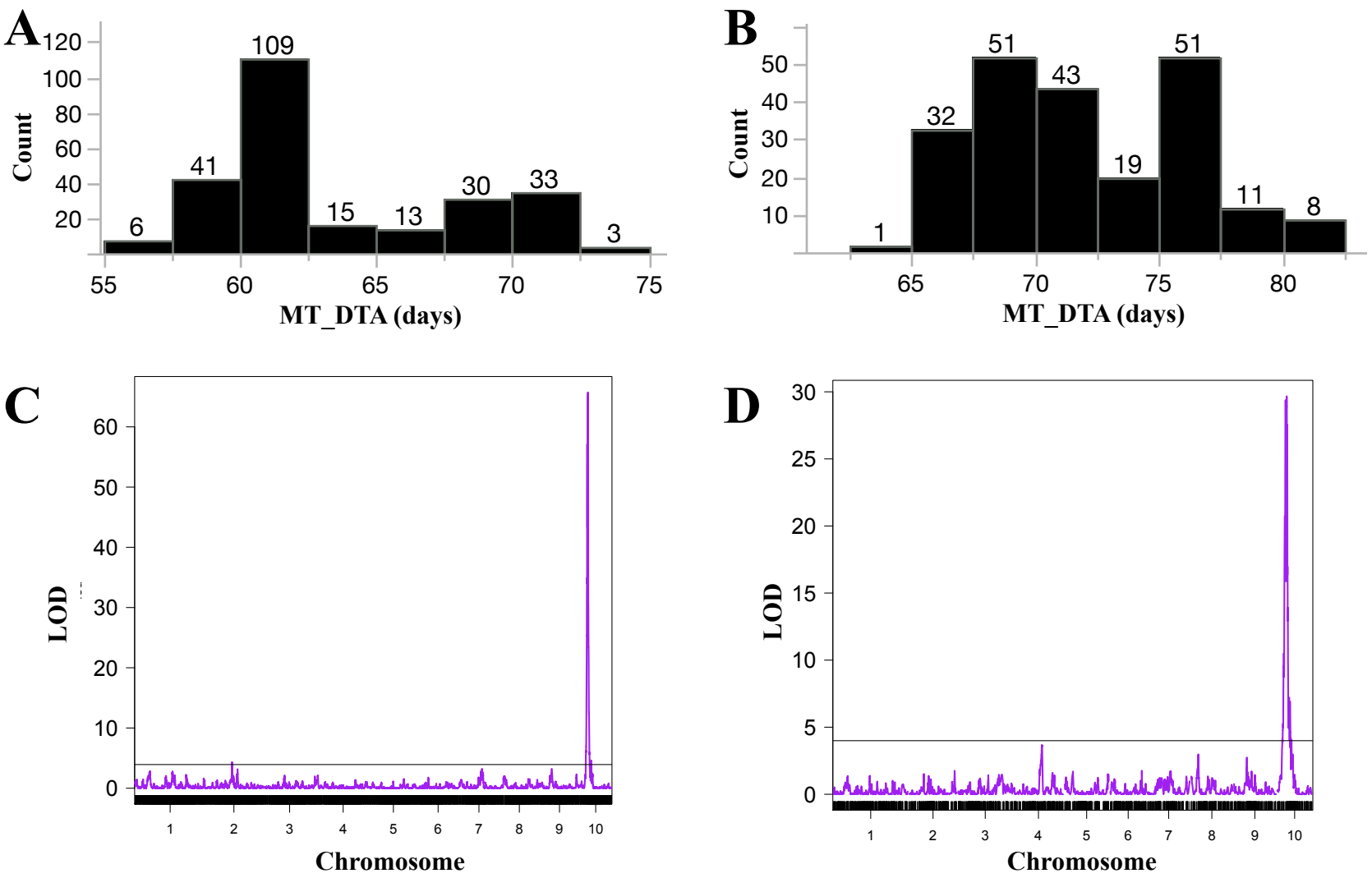

Figure 5. The distribution of days to 50% anthesis of the mutant siblings (MT_DTA) in (A) Syn10-DH x *Oy1-N1989/+*:B73, and (B) IBM-RILs x *Oy1-N1989/+*:B73 F_1 population. Genome-wide QTL plot of MT_DTA in (C) Syn10-DH, and (D) IBM-RILs F_1 population. The x-axis in (C) and (D) indicates the chromosome number, and y-axis indicates the logarithm of odds (LOD) of tested markers. Black horizontal bar indicates permutation testing based threshold for QTL detection.

Figure 6. Effect of *vey1* locus from B73 and Mo17 on flowering time in reciprocal isogenic backgrounds. Representative plants showing
(A) Delayed maturity of the heterozygous mutants in isogenic Mo17 (BC_7 generation) inbred background, compared to the wild-type siblings. Mutant and wild-type siblings in b030 (B73-like NIL with $vey1^{B73}$) shows early flowering while the isogenic B73 introgression of the $vey1^{Mo17}$ allele in b094 NIL exhibits delayed flowering.
(B) Early maturity in the heterozygous mutant in m097 (Mo17-like NIL with $vey1^{B73}$) compared to the mutant in B73 x Mo17 F_1 hybrid background. Measuring stick on the left in both panels is 243 cm.

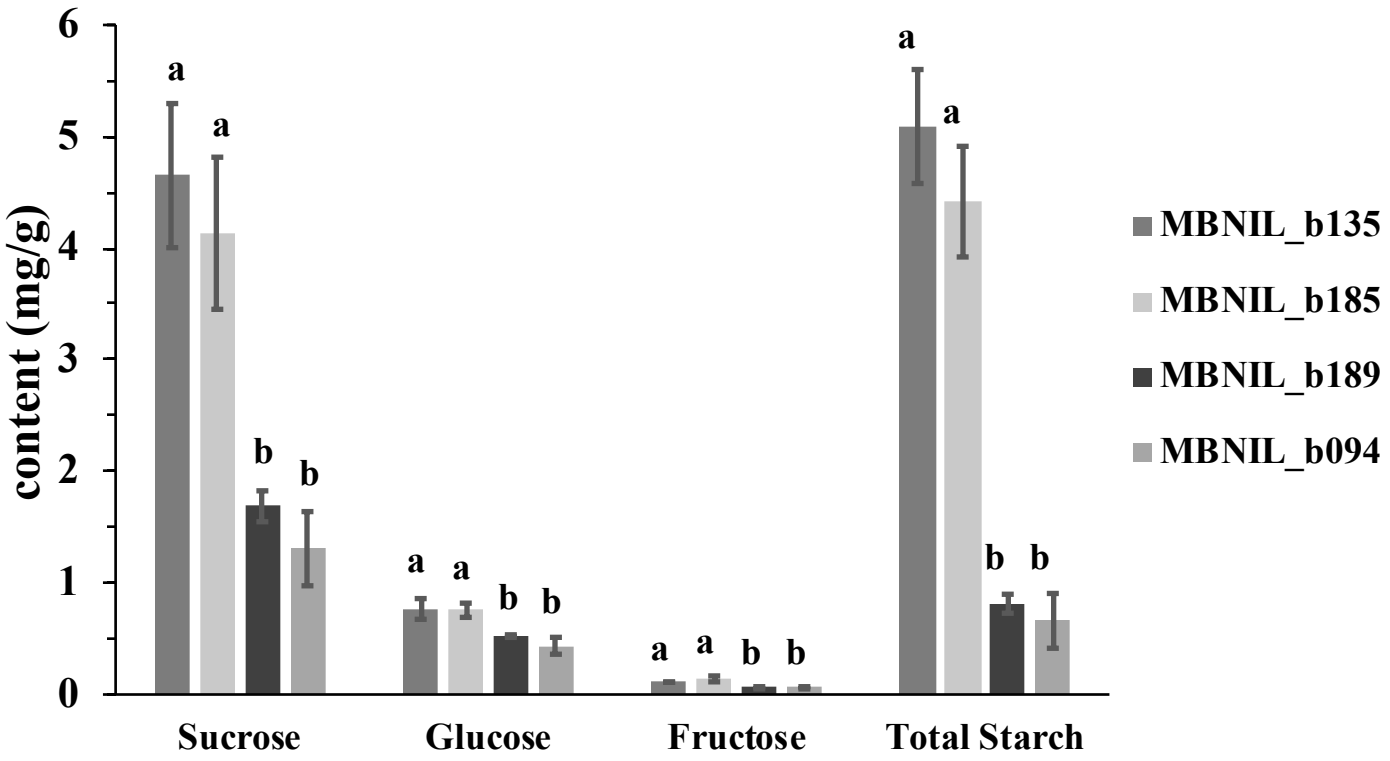

Figure 7. The effect of alleles at *vey1* on leaf soluble sugars and starch content in *Oy1-N1989/+* heterozygotes in the isogenic B73 background. B73-like NILs b135 and b185 have $vey1^{B73}$ introgression, whereas b189 and b094 have $vey1^{Mo17}$ introgression. The values of different sugars and starch are reported as mg/g of fresh weight.

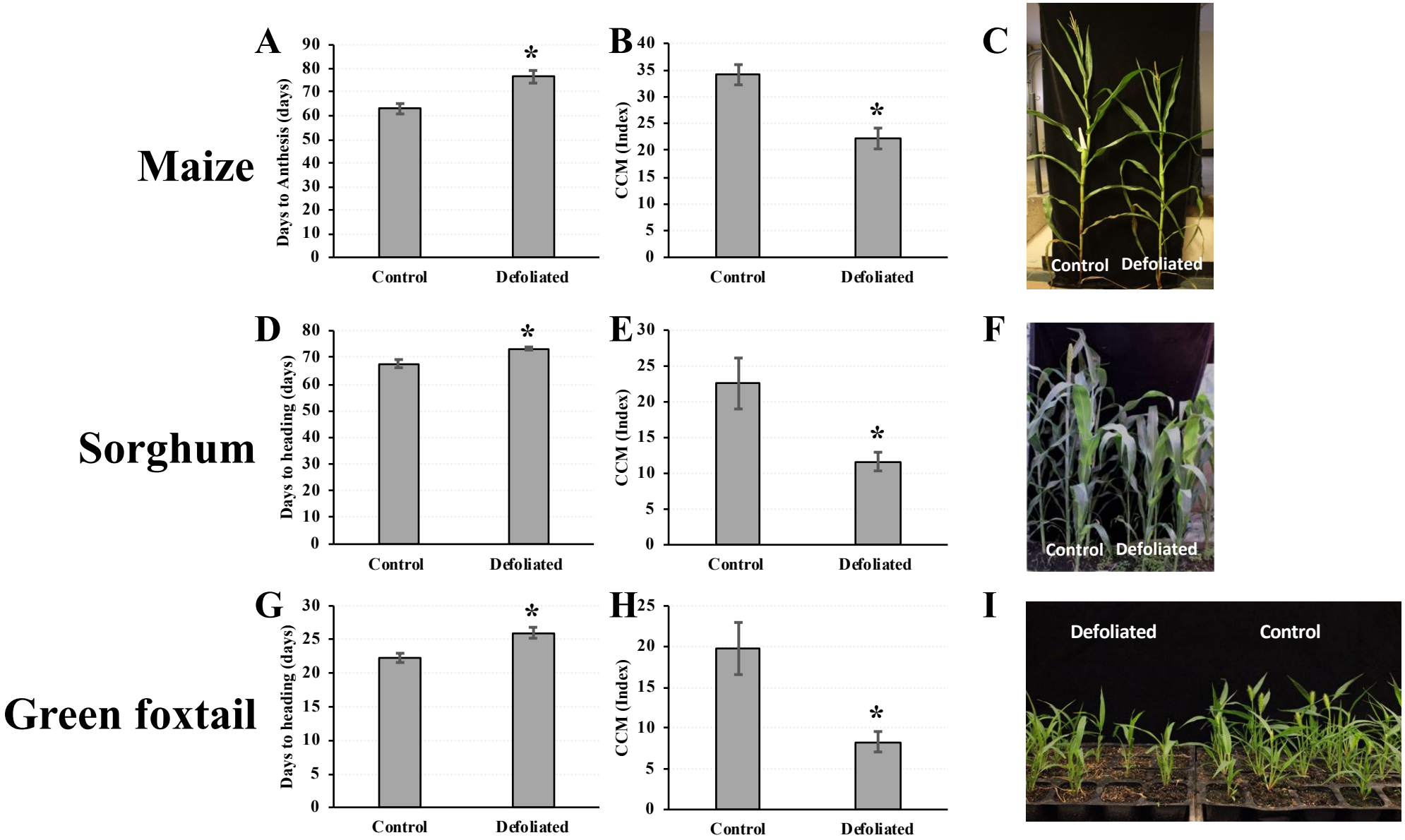

Figure 8. The effect of defoliation on flowering time and chlorophyll in the newly emerged leaves of (A-C) maize, (D-F) sorghum, and (G-I) green foxtail. The asterisk indicates significant difference between treatment means using student's t-test at $p<0.05$.

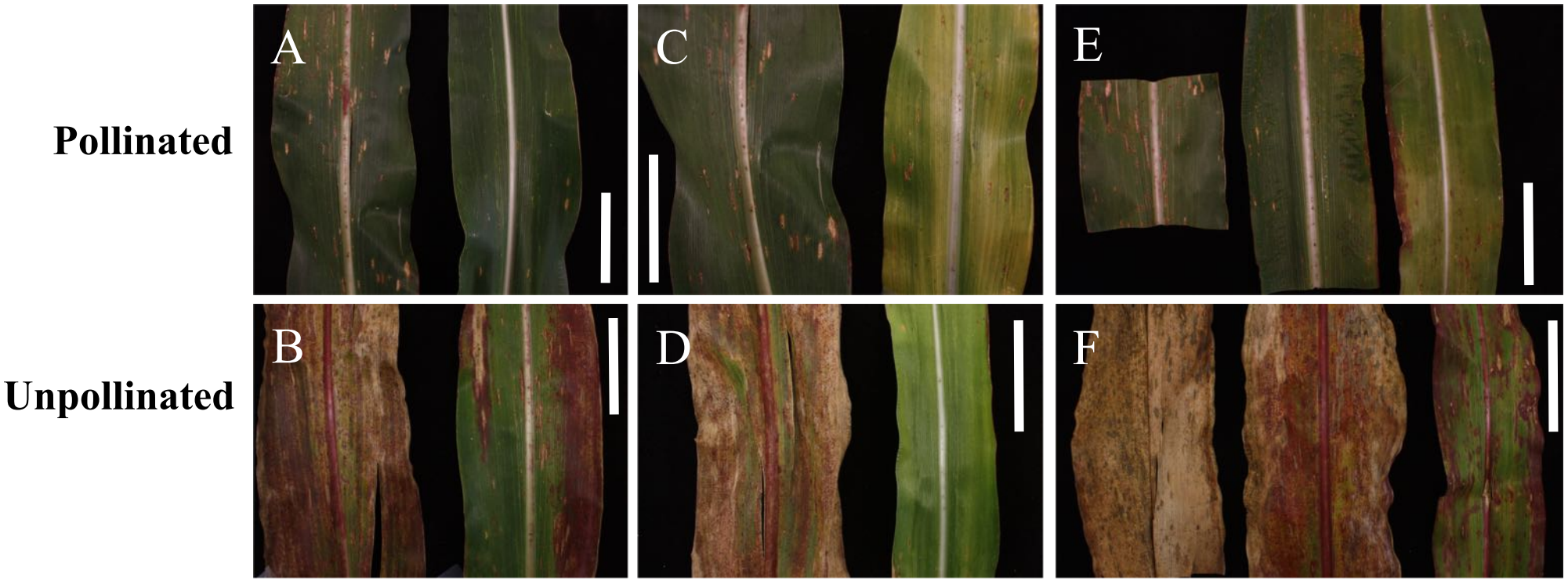

Figure 9. The effect of *vey1* on senescence induced by pollination prevention. Pictures of the representative primary ear leaf derived from plants at 30 and 40 days-after-anthesis (DAA) either with open pollinated (top panels: A, C, and E) or unpollinated (bottom panels: B, D, and F) ears. The representative primary ear leaf from (A-B) B73 wild-type (left) and mutant sibling (right) at 30DAA, (C-D) wild-type (left) and mutant (right) sibling from F_1 between B73-like NIL-b107 (with *vey1*^{Mo17} introgression) x *Oy1-N1989/+*:B73 at 30 DAA, (E-F) wild-type (B73-like NIL-b107), mutant B73-like NIL-b135 with *vey1*^{B73} (middle), and mutant B73-like NIL-b107 with *vey1*^{Mo17} allele (right) at 42 DAA. The scale bar in each figure is 6.35 cm.